A&A 606, A105 (2017)
DOI: 10.1051/0004-6361/201730383

Astronomy & Astrophysics

Stellar laboratories

IX. New Se V, Sr IV–VII, Te VI, and I VI oscillator strengths and the Se, Sr, Te, and I abundances in the hot white dwarfs G191−B2B and RE 0503−289⋆,⋆⋆,⋆⋆⋆

T. Rauch[1], P. Quinet[2,3], M. Knörzer[1], D. Hoyer[1], K. Werner[1], J. W. Kruk[4], and M. Demleitner[5]

[1] Institute for Astronomy and Astrophysics, Kepler Center for Astro and Particle Physics, Eberhard Karls University, Sand 1, 72076 Tübingen, Germany
e-mail: rauch@astro.uni-tuebingen.de
[2] Physique Atomique et Astrophysique, Université de Mons, UMONS, 7000 Mons, Belgium
[3] IPNAS, Université de Liège, Sart Tilman, 4000 Liège, Belgium
[4] NASA Goddard Space Flight Center, Greenbelt, MD 20771, USA
[5] Astronomisches Rechen-Institut (ARI), Centre for Astronomy of Heidelberg University, Mönchhofstraße 12-14, 69120 Heidelberg, Germany

Received 2 January 2017 / Accepted 17 June 2017

ABSTRACT

Context. To analyze spectra of hot stars, advanced non-local thermodynamic equilibrium (NLTE) model-atmosphere techniques are mandatory. Reliable atomic data is crucial for the calculation of such model atmospheres.
Aims. We aim to calculate new Sr IV–VII oscillator strengths to identify for the first time Sr spectral lines in hot white dwarf (WD) stars and to determine the photospheric Sr abundances. To measure the abundances of Se, Te, and I in hot WDs, we aim to compute new Se V, Te VI, and I VI oscillator strengths.
Methods. To consider radiative and collisional bound-bound transitions of Se V, Sr IV - VII, Te VI, and I VI in our NLTE atmosphere models, we calculated oscillator strengths for these ions.
Results. We newly identified four Se V, 23 Sr V, 1 Te VI, and three I VI lines in the ultraviolet (UV) spectrum of RE 0503−289. We measured a photospheric Sr abundance of $6.5^{+3.8}_{-2.4} \times 10^{-4}$ (mass fraction, 9500–23 800 times solar). We determined the abundances of Se ($1.6^{+0.9}_{-0.6} \times 10^{-3}$, 8000–20 000), Te ($2.5^{+1.5}_{-0.9} \times 10^{-4}$, 11 000–28 000), and I ($1.4^{+0.8}_{-0.5} \times 10^{-5}$, 2700–6700). No Se, Sr, Te, and I line was found in the UV spectra of G191−B2B and we could determine only upper abundance limits of approximately 100 times solar.
Conclusions. All identified Se V, Sr V, Te VI, and I VI lines in the UV spectrum of RE 0503−289 were simultaneously well reproduced with our newly calculated oscillator strengths.

Key words. atomic data – line: identification – stars: abundances – stars: individual: G191-B2B – stars: individual: RE 0503-289 – virtual observatory tools

1. Introduction

Recent spectral analyses (cf., Rauch et al. 2017) of high-resolution UV spectra of the helium-rich (DO-type) white dwarf (WD) RE 0503−289 (RX J0503.9−2854, WD 0501+527, McCook & Sion 1999a,b) revealed strongly enriched trans-iron elements (atomic numbers $Z \geq 30$) in its photosphere (Fig. 1). Efficient radiative levitation (Rauch et al. 2016a) in this hot WD (effective temperature $T_{\rm eff} = 70\,000 \pm 2000$ K, surface gravity $\log(g/{\rm cm\,s^{-2}}) = 7.5 \pm 0.1$, Rauch et al. 2016b) can increase abundances by more than 4 dex compared with solar values. In the cooler ($T_{\rm eff} = 60\,000 \pm 2000$ K, $\log g = 7.6 \pm 0.05$, Rauch et al. 2013), hydrogen-rich (DA-type) WD G191−B2B (WD 0501+527, McCook & Sion 1999a,b), the radiative levitation is able to retain only a factor of ≈100 fewer trans-iron elements in the photosphere than in RE 0503−289 (Fig. 1).

The search for signatures of trans-iron elements in the spectra of RE 0503−289 and G191−B2B was initiated by the discovery of Ga, Ge, As, Se, Kr, Mo, Sn, Te, I, and Xe lines in RE 0503−289 (Werner et al. 2012b). Subsequent calculations of transition probabilities allowed reliable abundance determinations of Zn (atomic number $Z = 30$), Ga (31), Ge (32), Kr (36), Zr (40), Mo (42), Xe (54), and Ba (56) (e.g., Rauch et al. 2017, and references therein). Based on the wavelengths provided by the Atomic Spectra Database (ASD[1]) of the National Institute of Standards and Technology (NIST), we have identified some strong lines of strontium (38), an element that was hitherto not detected in hot WDs. For an identification of other, weaker Sr lines and a subsequent abundance analysis, we decided to calculate new Sr IV-VII transition probabilities.

The paper is organized as follows. We briefly introduce the UV spectra in Sect. 2. Our model atmospheres, the atomic data

⋆ Based on observations with the NASA/ESA *Hubble* Space Telescope, obtained at the Space Telescope Science Institute, which is operated by the Association of Universities for Research in Astronomy, Inc., under NASA contract NAS5-26666.
⋆⋆ Based on observations made with the NASA-CNES-CSA Far Ultraviolet Spectroscopic Explorer.
⋆⋆⋆ Full Tables A.15 to A.21 are only available via the German Astrophysical Virtual Observatory (GAVO) service TOSS (http://dc.g-vo.org/TOSS).

[1] http://physics.nist.gov/PhysRefData/ASD/lines_form.html

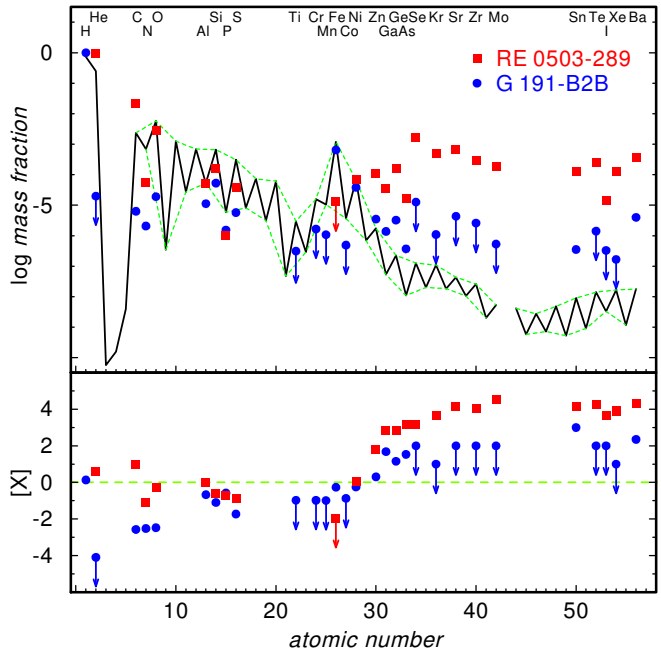

Fig. 1. Solar abundances (Asplund et al. 2009; Scott et al. 2015a,b; Grevesse et al. 2015, thick line; the dashed lines connect the elements with even and with odd atomic number) compared with the determined photospheric abundances of RE 0503−289 (red squares, Dreizler & Werner 1996; Rauch et al. 2012, 2014a,b, 2015, 2016a,b, 2017, and this work). The uncertainties of the WD abundances are about 0.2 dex in general. Arrows indicate upper limits. *Top panel*: abundances given as logarithmic mass fractions. *Bottom panel*: abundance ratios to respective solar values, [X] denotes log (fraction/solar fraction) of species X. The dashed, green line indicates solar abundances.

as well as the transition-probability calculations are described in Sect. 3. Here, we have included the calculation of new transition probabilities for Se V, Te VI, and I VI because these are the last three elements (34, 52, and 53, respectively), that were previously identified by Werner et al. (2012b) in the spectrum of RE 0503−289. The line identification and abundance analysis then follows in Sect. 4.

2. Observations

Our analysis is based on UV spectroscopy that was performed with the Far Ultraviolet Spectroscopic Explorer (FUSE, 910 Å $< \lambda <$ 1190 Å, resolving power $R \approx 20\,000$) and the *Hubble* Space Telescope/Space Telescope Imaging Spectrograph (HST/STIS, 1144 Å $< \lambda <$ 1709 Å, $R \approx 45\,800$). The spectra are described in detail in Hoyer et al. (2017). The observed spectra shown here were shifted to rest wavelengths, using $v_{\rm rad} = 24.56\,{\rm km\,s^{-1}}$ for G191−B2B (Lemoine et al. 2002) and $25.8\,{\rm km\,s^{-1}}$ for RE 0503−289 (Hoyer et al. 2017). To compare them with our synthetic spectra, the latter were convolved with Gaussians to model the respective instruments' resolving power.

3. Model atmospheres and atomic data

To calculate model atmospheres for our analysis, we used the Tübingen Model-Atmosphere Package (TMAP[2], Werner et al. 2003, 2012a). These models are plane-parallel, chemically homogeneous, and in hydrostatic and radiative equilibrium. TMAP considers non-local thermodynamic equilibrium (NLTE). More details are given by Rauch et al. (2016b). We include opacities of H^G, He, C, N, O, Al, Si, P, S, Ca, Sc, Ti, V, Cr, Mn, Fe, Co, Ni, Zn, Ga, Ge, As, Se, Kr^R, Sr, Zr, Mo, Sn, Te, I, Xe^R, and Ba (^{G}: only in G191−B2B models, ^{R}: only in RE 0503−289 models). Model atoms for all species with $Z < 20$ are compiled from the Tübingen Model Atom Database (TMAD). For the iron-group elements (Ca – Ni, $20 \le Z \le 28$), model atoms were constructed with a statistical approach by calculating so-called super levels and super lines (IrOnIc code, Rauch & Deetjen 2003) with the Tübingen Iron-Group Opacity – IrOnIc WWW Interface (Müller-Ringat 2013). For trans-iron elements ($Z \ge 29$), we transferred their atomic data into Kurucz-formatted files (cf., Rauch et al. 2015), and followed the same statistical method. The Se, Sr, Te, and I model-atom statistics are given in Table 1.

Table 1. Statistics of the Se V, Sr IV–VII, Te VI, and I VI atomic levels and line transitions from Tables A.15–A.21.

Ion	Atomic levels	Lines	Super levels	Super lines
Se V	46	310	7	19
Sr IV	254	7578	7	21
Sr V	130	2022	7	19
Sr VI	22	70	7	10
Sr VII	19	46	7	10
Te VI	30	178	7	12
I VI	38	197	7	15

New sets of oscillator strengths and transition probabilities for the Se V, Sr IV-VII, Te VI, and I VI ions were computed using the pseudo-relativistic Hartree-Fock (HFR) approach of Cowan (1981) modified for including core-polarization effects, giving rise to the HFR+ CPOL method, as described by Quinet et al. (1999, 2002). For each ion, this method was combined with a semi-empirical least-squares fit of radial energy parameters to minimize the differences between computed and available experimental energy levels.

Se V: the $4s^2$, $4p^2$, $4d^2$, $4f^2$, 4s4d, 4s5d, 4s6d, 4s5s, 4s6s, 4p4f, 4p5f, 4p6f, 4d5s, 4d6s, 4d5d, and 4d6d even-parity configurations and the 4s4p, 4s5p, 4s6p, 4s4f, 4s5f, 4s6f, 4p4d, 4p5d, 4p6d, 4p5s, 4p6s, 4d4f, and 4d5f odd-parity configurations were explicitly included in the physical model. Core-polarization effects were estimated by assuming a Ni-like Se VII ionic core with a core-polarizability $\alpha_{\rm d}$ of 0.36 au, as reported by Johnson et al. (1983), and a cut-off radius, $r_{\rm c}$ equal to 0.62 au, corresponding to the HFR mean radius of the outermost core orbital (3d). Using the experimental energy levels published by Churilov & Joshi (1995), the radial integrals characterizing the $4s^2$, $4p^2$, 4s4d, 4s5d, 4s5s, 4s6s, 4s4p, 4s5p, 4s4f, 4p4d, and 4p5s configurations were fitted. This semi-empirical adjustment allowed us to reduce the average deviations between calculated and measured energies to $8\,{\rm cm^{-1}}$ and $219\,{\rm cm^{-1}}$ for even and odd parities, respectively.

Sr IV: we considered interaction among the configurations $4s^24p^5$, $4s^24p^45p$, $4s^24p^46p$, $4s^24p^44f$, $4s^24p^45f$, $4s^24p^46f$, $4s^24p^46h$, $4s4p^54d$, $4s4p^55d$, $4s4p^56d$, $4s4p^55s$, $4s4p^56s$, $4s4p^55g$, $4s4p^56g$, $4s^24p^34d^2$, $4s^24p^34f^2$, and $4p^64f$ for the odd parity, and $4s4p^6$, $4s^24p^44d$, $4s^24p^45d$, $4s^24p^46d$, $4s^24p^45s$, $4s^24p^46s$, $4s^24p^47s$, $4s^24p^45g$, $4s^24p^46g$, $4s4p^54f$, $4s4p^55f$, $4s4p^56f$, $4s4p^55p$, $4s4p^56p$, $4s4p^56h$, $4p^64d$, and $4p^65s$ for the even parity. The core-polarization parameters were the dipole

[2] http://astro.uni-tuebingen.de/~TMAP

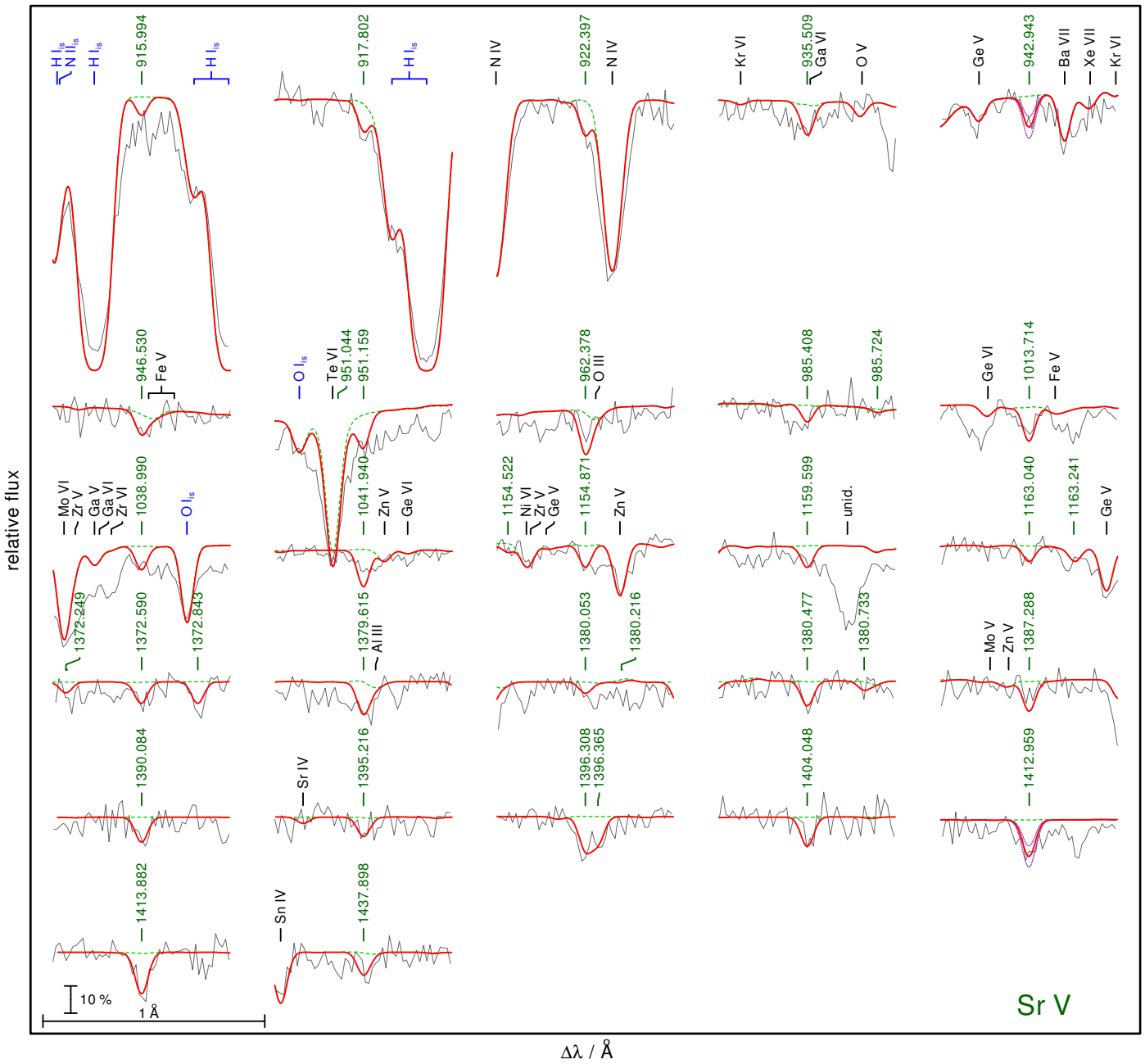

Fig. 2. Sr V lines in the observation (gray line) of RE 0503−289, labeled with their wavelengths from Table A.17. The thick, red spectrum is calculated from our best model with a Sr mass fraction of 6.5×10^{-4}. The dashed, green line shows a synthetic spectrum calculated without Sr. In cases of Sr V λ 942.943 Å and Sr V λ 1412.959 Å, the red, dashed lines show two synthetic spectra calculated with Sr abundances that were increased and decreased by 0.3 dex. The vertical bar indicates 10% of the continuum flux. Identified lines are marked. "is" denotes interstellar.

polarizability of a Ni-like Sr IX ionic core as reported by Johnson et al. (1983), that is, $\alpha_d = 0.13$ au, and the cut-off radius corresponding to the HFR mean value $\langle r \rangle$ of the outermost core orbital (3d), i.e., $r_c = 0.49$ au. Using experimental energy levels compiled by Sansonetti (2012), the radial integrals (average energy, Slater, spin-orbit and effective interaction parameters) of $4p^5$, $4p^45p$, $4p^46p$, $4p^44f$, $4p^45f$, $4p^46h$, $4s4p^54d$, $4s4p^6$, $4p^44d$, $4p^45d$, $4p^46d$, $4p^45s$, $4p^46s$, $4p^47s$, $4p^45g$, and $4p^46g$ configurations were optimized by a least-squares fitting procedure in which the mean deviations with experimental data were found to be equal to 145 cm^{-1} for the odd parity and 150 cm^{-1} for the even parity.

Sr V: the HFR method was used with, as interacting configurations, $4s^24p^4$, $4s^24p^35p$, $4s^24p^36p$, $4s^24p^34f$, $4s^24p^35f$, $4s^24p^36f$, $4s^24p^36h$, $4s4p^44d$, $4s4p^45d$, $4s4p^46d$, $4s4p^45s$, $4s4p^46s$, $4s4p^45g$, $4s4p^46g$, $4s^24p^24d^2$, $4s^24p^24f^2$, $4p^6$, and $4p^54f$ for the even parity, and $4s4p^5$, $4s^24p^34d$, $4s^24p^35d$, $4s^24p^36d$, $4s^24p^35s$, $4s^24p^36s$, $4s^24p^35g$, $4s^24p^36g$, $4s4p^44f$, $4s4p^45f$, $4s4p^46f$, $4s4p^45p$, $4s4p^46p$, $4s4p^46h$, $4p^54d$, and $4p^55s$ for the odd parity. Core-polarization effects were estimated using the same α_d and r_c values as those considered in Sr IV. The radial integrals corresponding to $4p^4$, $4p^35p$, $4s4p^5$, $4p^34d$, $4p^35d$, $4p^35s$, and $4p^36s$ were adjusted to reproduce at best the experimental energy levels tabulated by Sansonetti (2012). We note

that the few levels reported by this author as belonging to the $4p^3 4f$ and $4p^3 5f$ configurations were not included in the fitting process because it was found that most of those levels were strongly mixed with states of experimentally unknown configurations, such as $4s4p^4 4d$, $4p^3 6p$, $4p^2 4d^2$, and $4s4p^4 5s$. It was then extremely difficult to establish an unambiguous correspondence between the calculated and experimental energies. For the levels considered in our semi-empirical adjustment, we found mean deviations equal to 138 cm^{-1} and 231 cm^{-1} in even and odd parities, respectively.

Sr VI: the configurations included in the HFR model were $4s^2 4p^3$, $4s^2 4p^2 5p$, $4s^2 4p^2 6p$, $4s^2 4p^2 4f$, $4s^2 4p^2 5f$, $4s^2 4p^2 6f$, $4s^2 4p^2 6h$, $4s4p^3 4d$, $4s4p^3 5d$, $4s4p^3 6d$, $4s4p^3 5s$, $4s4p^3 6s$, $4s4p^3 5g$, $4s4p^3 6g$, $4s^2 4p4d^2$, $4s^2 4p4f^2$, $4p^5$, and $4p^4 4f$ for the odd parity, and $4s4p^4$, $4s^2 4p^2 4d$, $4s^2 4p^2 5d$, $4s^2 4p^2 6d$, $4s^2 4p^2 5s$, $4s^2 4p^2 6s$, $4s^2 4p^2 5g$, $4s^2 4p^2 6g$, $4s4p^3 4f$, $4s4p^3 5f$, $4s4p^3 6f$, $4s4p^3 5p$, $4s4p^3 6p$, $4s4p^3 6h$, $4p^4 4d$, and $4p^4 5s$ for the even parity. The same core-polarization parameters as those used for Sr IV were considered while the fitting process was performed with the few experimental energy levels listed in the compilation of Sansonetti (2012) for optimizing the radial parameters of $4p^3$, $4s4p^4$, and $4p^2 5s$ configurations, leading to mean deviations equal to 13 cm^{-1} (odd parity) and 32 cm^{-1} (even parity).

Sr VII: a model similar to that of Sr VI was used, for which the $4s^2 4p^2$, $4s^2 4p5p$, $4s^2 4p6p$, $4s^2 4p4f$, $4s^2 4p5f$, $4s^2 4p6f$, $4s^2 4p6h$, $4s4p^2 4d$, $4s4p^2 5d$, $4s4p^2 6d$, $4s4p^2 5s$, $4s4p^2 6s$, $4s4p^2 5g$, $4s4p^2 6g$, $4s^2 4d^2$, $4s^2 4f^2$, $4p^4$, and $4p^3 4f$ even-parity configurations and the $4s4p^3$, $4s^2 4p4d$, $4s^2 4p5d$, $4s^2 4p6d$, $4s^2 4p5s$, $4s^2 4p6s$, $4s^2 4p5g$, $4s^2 4p6g$, $4s4p^2 4f$, $4s4p^2 5f$, $4s4p^2 6f$, $4s4p^2 5p$, $4s4p^2 6p$, $4s4p^2 6h$, $4p^3 4d$, and $4p^3 5s$ odd-parity configurations were explicitly included in the HFR model. Here also, we used the same core-polarization parameters as those considered for Sr IV. The semi-empirical optimization process was carried out to adjust the radial parameters in $4p^2$, $4s4p^3$, and 4p5s with the experimental energy levels taken from Sansonetti (2012) giving rise to average deviations of 0 cm^{-1} and 247 cm^{-1} for even and odd parities, respectively.

Te VI: the configuration interaction was considered among the following configurations: $4d^{10}5s$, $4d^{10}6s$, $4d^{10}7s$, $4d^{10}5d$, $4d^{10}6d$, $4d^{10}7d$, $4d^9 5s^2$, $4d^9 5p^2$, $4d^9 5d^2$, $4d^9 4f^2$, $4d^9 5s5d$, $4d^9 5s6d$, $4d^9 5s6s$, $4d^9 4f5p$, and $4d^9 4f6p$ (even parity) and $4d^{10}5p$, $4d^{10}6p$, $4d^{10}7p$, $4d^{10}4f$, $4d^{10}5f$, $4d^{10}6f$, $4d^{10}7f$, $4d^9 5s5p$, $4d^9 5s6p$, $4d^9 5s5f$, $4d^9 5s6f$, $4d^9 4f5s$, $4d^9 4f6s$, $4d^9 4f5d$, $4d^9 4f6d$ (odd parity). The core-polarization parameters were those corresponding to a Rh-like Te VIII ionic core, that is, α_d = 1.15 au (Fraga et al. 1976) and $r_c \equiv \langle r \rangle_{4d}$ = 0.95 au. The radial parameters of $4d^{10}5s$, $4d^{10}6s$, $4d^{10}5d$, $4d^9 5p^2$, $4d^{10}5p$, $4d^{10}6p$, and $4d^9 5s5p$ configurations were optimized to minimize the differences between the computed Hamiltonian eigenvalues and the experimental energy levels published by Crooker & Joshi (1964), Dunne & O'Sullivan (1992), and Ryabtsev et al. (2007) giving rise to mean deviations of 89 m^{-1} (even parity) and 13 cm^{-1} (odd parity).

I VI: thirty-two configurations were included in the HFR model used to compute the atomic structure, i.e., $5s^2$, $5p^2$, $5d^2$, $4f^2$, $5f^2$, 5s5d, 5s6d, 5s7d, 5s6s, 5s7s, 5p4f, 5p5f, 5p6f, 5d6s, 5d7s, 5d6d, and 5d7d for the even parity and 5s5p, 5s6p, 5s7p, 5s4f, 5s5f, 5s6f, 5s7f, 5p5d, 5p6d, 5p7d, 5p6s, 5p7s, 5d4f, 5d5f, and 5d6f for the odd parity. An ionic core of the type Pd-like I VIII was considered to estimate the core-polarization effects with the parameters α_d = 1.03 a.u. (Johnson et al. 1983) and $r_c \equiv \langle r \rangle_{4d}$ = 0.90 au. The semi-empirical optimization process was carried out to adjust the radial parameters in $5s^2$, $5p^2$, 5s5d, 5s6s, 5s7s, 5s5p, 5s6p, 5p5d, and 5p6s with the experimental energy levels taken from Tauheed et al. (1997) giving rise to average deviations of 72 cm^{-1} and 175 cm^{-1} for even and odd parities, respectively.

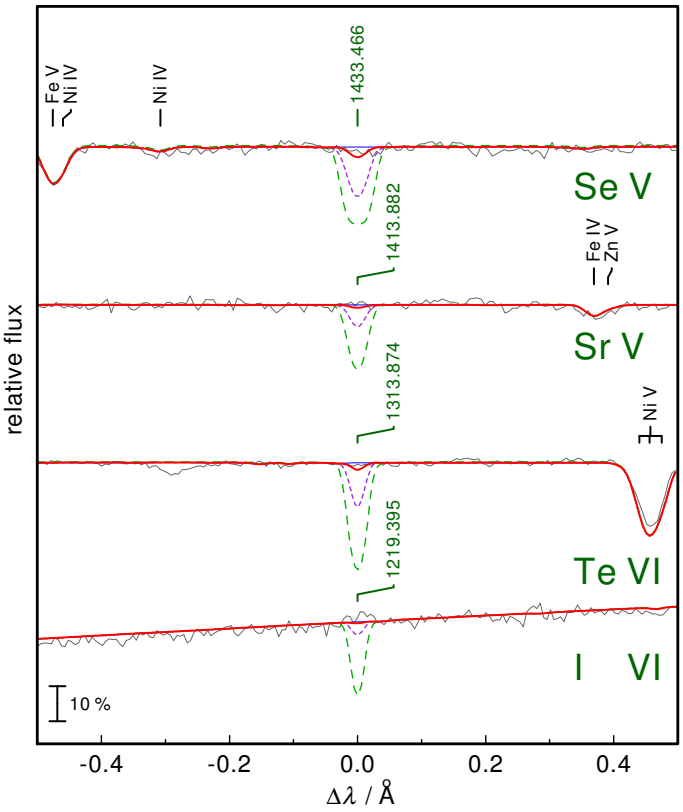

Fig. 3. STIS observation of G191−B2B (gray) compared with synthetic line profiles of Se V λ 1433.466 Å, Sr V λ 1413.882 Å, Te VI λ 1313.874 Å, and I VI λ 1219.395 Å. The models were calculated with four abundances of the respective elements, without (thin, blue), with 100 times (thick, red), 1000 times (short dashed, violet) and 10 000 times solar abundance (long dashed, green).

The parameters adopted in our computations are summarized in Tables A.1–A.7 while calculated and available experimental energies are compared in Tables A.8–A.14, for Se V, Sr IV-VII,Te VI, and I VI, respectively. Tables A.15–A.21 give the newly computed weighted oscillator strengths ($\log g_i f_{ik}$, i and k are the indexes of the lower and upper energy level, respectively) and transition probabilities ($g_k A_{ki}$, in s^{-1}) together with the numerical values (in cm^{-1}) of the lower and upper energy levels and the corresponding wavelengths (in Å). In the final column of each table, we also give the cancellation factor, CF, as defined by Cowan (1981). We note that very low values of this factor (typically <0.05) indicate strong cancellation effects in the calculation of line strengths. In these cases, the corresponding $\log g_i f_{ik}$ and $g_k A_{ki}$ values could be very inaccurate and therefore need to be considered with some care. Figure B.1 shows the

newly calculated $\log g_i f_{ik}$ values from the X-ray to the far infrared wavelength range.

Radiative decay rates for some transitions in the same ions as those considered in the present work were reported in previous papers. More precisely, for Se V, large-scale calculations for the $4s^2$–4s4p transitions were performed by Liu et al. (2006) using the multiconfiguration Dirac-Fock (MCDF) method and by Chen & Cheng (2010) using B-spline basis functions while the Relativistic Many Body Perturbation Theory (RMBPT), including the Breit interaction was used by Safronova & Safronova (2010) to compute oscillator strengths for transitions between even-parity $4s^2$, $4p^2$, 4s4d, $4d^2$, 4p4f, $4f^2$ and odd-parity 4s4p, 4s4f, 4p4d, 4d4f states. In Sr IV, transition probabilities and oscillator strengths for the electric dipole transitions involving the $4s^24p^5$, $4s^24p^44d$ and $4s4p^6$ configurations were obtained using the multiconfiguration Dirac-Fock approach by Singh et al. (2013) and by Aggarwal & Keenan (2014). These works were subsequently extended by Aggarwal & Keenan (2015) to transitions involving the $4s^24p^5$, $4s^24p^44\ell$, $4s4p^6$, $4s^24p^45\ell$, $4s^24p^34d^2$, $4s4p^54\ell$, and $4s4p^55\ell$ configurations. For Sr VI, relativistic quantum defect orbital (RQDO) and MCDF calculations of oscillator strengths were carried out by Charro & Martín (1998, 2005) for the $4p^3$–$4p^25s$ transition array while the same methods were used by Charro & Martín (2002, 2005) for investigating the $4p^2$–4p5s transitions in Sr VII. In the case of Te VI, Chou & Johnson (1997) performed third-order relativistic many-body perturbation theory (MBPT) calculations to evaluate the rates for 5s–5p transitions while Migdalek & Garmulewicz (2000) used a relativistic ab initio model potential approach with explicit local exchange to produce oscillator strengths. In the same ion, the 5s–5p transition rates were also computed by Głowacki & Migdałek (2009) who employed a configuration-interaction method with numerical Dirac-Fock wave functions generated with noninteger outermost core shell occupation number while transition probabilities for 5s–5p, 5p–5d, 4f–5d, and 5d–5f transitions were calculated by Ivanova (2011). Finally, for I VI, the oscillator strengths of the allowed and spin-forbidden $5s^2\ {}^1S_0$–$5s5p\ {}^{1,3}P_1$ transitions were evaluated by Biémont et al. (2000) using the relativistic Hartree-Fock approach, including a core-polarization potential, and the MCDF method, as well as by Glowacki & Migdalek (2003) who used a relativistic configuration-interaction method with numerical Dirac-Fock wavefunctions generated with an ab initio model potential allowing for core-valence correlation.

In order to estimate the overall reliability of the new atomic data obtained in the present work, we have compared them with some of the most recent and the most extensive calculations available in literature, selected among those listed hereabove. More particularly, in Se V, we noticed that our oscillator strengths were in excellent agreement (within a few percent) with the RMBPT values published by Safronova & Safronova (2010). In the case of Sr IV, we found a general agreement of about 20−30% between our results and the oscillator strengths published by Aggarwal & Keenan (2015), this agreement reaching even 10% for the most intense lines. For Te VI, the mean ratio between our transition probabilities and the few values reported by Ivanova (2011) was found to be equal to 1.18 while, for I VI, a very good agreement (within 10%) was observed when comparing the gf-values obtained in the present work with those computed by Biémont et al. (2000) using either a relativistic Hartree-Fock or an MCDF model, taking core-valence correlation effects into account. All these comparisons allowed us to conclude that the accuracy of the new atomic data listed in the present paper should be about 20%, at least for the strongest lines.

Table 2. Identified Se V, Sr V, Te VI, and I VI lines in the UV spectrum of RE 0503−289.

Ion	Wavelength/Å	Comment
Sr V	915.994	uncertain
Sr V	917.802	
I VI	919.210	blend, uncertain
I VI	919.555	blend, uncertain
Sr V	922.397	
Sr V	935.509	blend, weak Ga VI
Sr V	942.943	
Sr V	946.530	
Te VI	951.021[a]	
Sr V	951.044	blend, strong Te VI
Sr V	951.159	
Sr V	962.378	blend, weak O III
Sr V	985.408	uncertain
Sr V	1013.714	
Sr V	1038.990	
Sr V	1041.940	
I VI	1053.389	weak
I VI	1057.530	blend, strong Zn V
Te VI	1071.414[a]	
Se V	1094.691[a]	
I VI	1120.301[a]	
Se V	1150.986[a]	shifted[b] to 1151.016 Å
I VI	1153.262	
Sr V	1154.871	
Sr V	1159.599	uncertain
Sr V	1163.040	
Se V	1227.446	shifted[c] to 1227.540 Å
Te VI	1313.874	
Sr V	1372.590	
Sr V	1372.843	
Sr V	1379.615	blend, weak Al III
Sr V	1380.053	uncertain
Sr V	1380.477	
Sr V	1387.288	uncertain
Sr V	1390.084	
Sr V	1395.216	uncertain
Sr V	1396.308	blend, Sr V λ 1396.365 Å
Sr V	1396.365	blend, Sr V λ 1396.308 Å
Sr V	1404.048	
Sr V	1412.958	
Sr V	1413.882	
Sr V	1437.898	
Se V	1451.779	shifted[d] to 1451.653 Å
Se V	1454.292	

Notes. The wavelengths correspond to those in Table A.17. [(a)] Identified by Werner et al. (2012b), [(b)] shifted to match observation. Rao & Badami (1931) measured 1151.96 Å, [(c)] shifted to match observation. Rao & Badami (1931) measured 1227.58 Å, [(d)] shifted to match observation.

4. Results

In the FUSE and HST/STIS observations of RE 0503−289, we newly identified 23 Sr V lines, listed in Table 2 which complements Table A.1 of Hoyer et al. (2017). Many more weak Sr V lines are visible in our model spectra that are not detectable in the noise of the available observations. The models show that the strongest Sr VI lines are located in the extreme ultraviolet

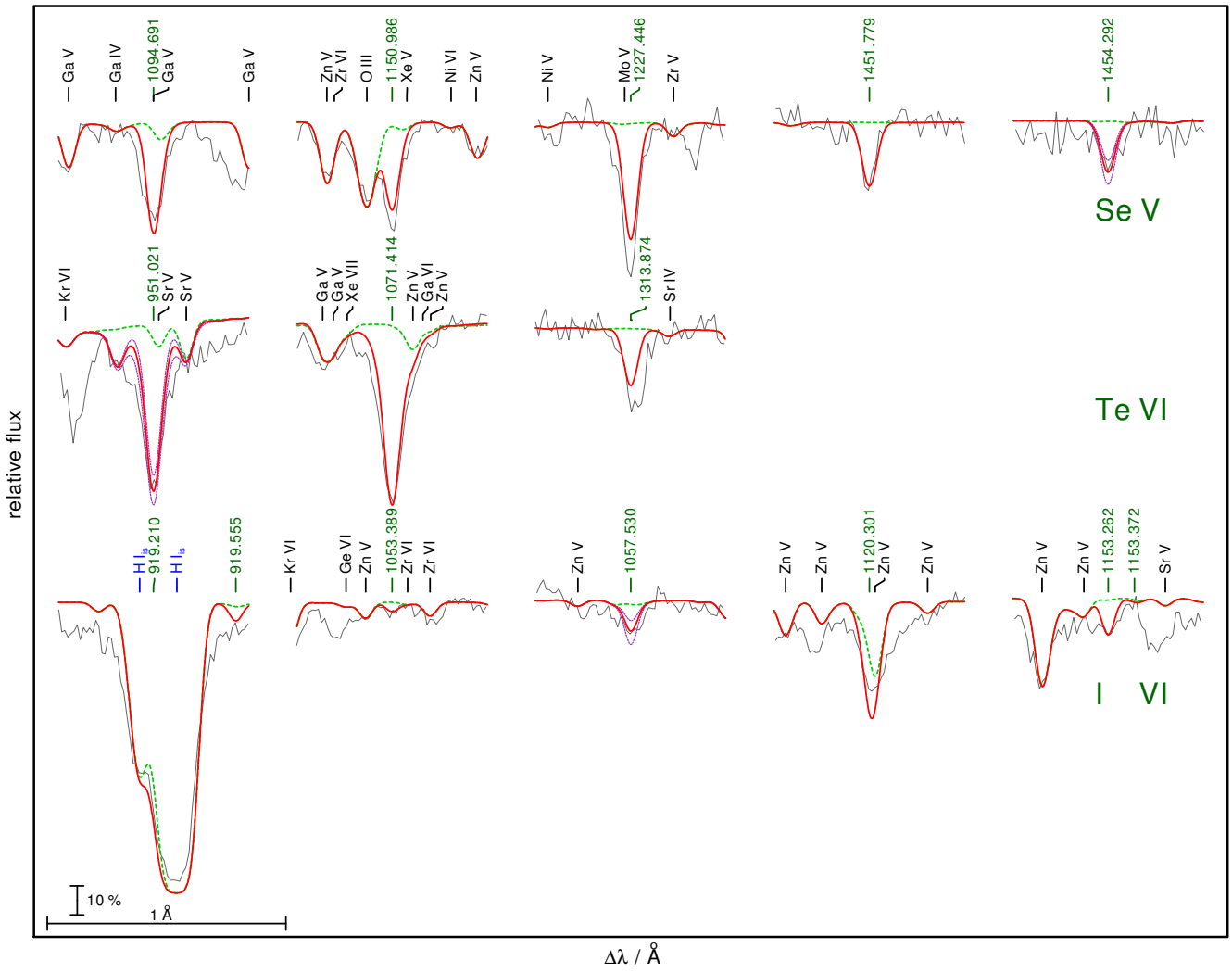

Fig. 4. As Fig. 2, for Se V (*top*, mass fraction of $1.6 \pm 1.0 \times 10^{-3}$ in the model), Te VI (*middle*, 2.5×10^{-4}), and I VI (*bottom*, 1.4×10^{-5}) lines. Abundance dependencies (±0.3 dex, red, dashed lines) are demonstrated for Se V λ 1454.292 Å, Te VI λ 951.021 Å, and I VI λ 1057.530 Å.

(EUV) and X-ray wavelength range while Sr IV lines are too weak in general and fade within the noise of the available observations. The observed Sr V lines are well reproduced by our model calculated with a mass fraction of 6.5×10^{-4} (Fig. 2). To estimate the abundance uncertainty from the error propagation of $T_{\rm eff}$ and $\log g$, we evaluated models at the error limits ($T_{\rm eff} = 70\,000 \pm 2000$ K, $\log g = 7.5 \pm 0.1$) and found that it is smaller than 0.1 dex. To consider the abundance uncertainties of other metals and the impact of their background opacities, we finally adopted a Sr mass fraction of 6.5×10^{-4} with an uncertainty of 0.2 dex (Fig. 2 shows exemplarily the abundance dependence of two lines in a [−0.3 dex, +0.3 dex] abundance interval). The determined Sr abundance matches well the abundance pattern of trans-iron elements in RE 0503−289 (Fig. 1). Their extreme overabundances are the result of efficient radiative levitation (Rauch et al. 2016a).

Five Se V, three Te VI, and four I VI lines are used for the abundance determination of these elements (Fig. 4). We measured mass fractions of 1.6×10^{-3}, 2.5×10^{-4}, and 1.4×10^{-5} for Se, Te, and I, respectively. These agree well with the expectations from the abundance pattern of trans-iron elements in RE 0503−289 (Fig. 1).

A very weak impact of Se, Sr, Te, and I lines is noticeable in the EUV wavelength range. The so-called EUV problem, that is, the flux discrepancy between model and observation in this wavelength range (cf., Hoyer et al. 2017) is, however, not significantly reduced. We note that Preval et al. (2017) showed recently that improved, larger photoionization cross-section of Ni can reduce this discrepancy.

The search for Se, Sr, Te, and I lines in the FUSE and HST/STIS observations of G191−B2B was entirely negative. Figure 3 shows the most prominent lines that are predicted by our models, namely Se V λ 1433.466 Å ($\log g_i f_{ik}$ value of 0.16), Sr V λ 1413.882 Å (0.82), Te VI λ 1313.874 Å (−0.05), and I VI λ 1219.395 Å (−0.63). For all these elements, the upper abundance limit is ≈100 times the solar abundance.

Acknowledgements. T.R. and D.H. are supported by the German Aerospace Center (DLR, grants 05 OR 1507 and 50 OR 1501, respectively). The GAVO project had been supported by the Federal Ministry of Education and Research (BMBF) at Tübingen (05 AC 6 VTB, 05 AC 11 VTB) and is funded at Heidelberg (05 AC 11 VH3). Financial support from the Belgian FRS-FNRS is also acknowledged. P.Q. is research director of this organization. Some of the data presented in this paper were obtained from the Mikulski Archive for Space Telescopes (MAST). STScI is operated by the Association of Universities for Research in Astronomy, Inc., under NASA contract NAS5-26555. Support for MAST for non-HST data is provided by the NASA Office of Space Science via grant NNX09AF08G and by other grants and contracts. The TIRO (http://astro.uni-tuebingen.de/~TIRO), TMAD (http://astro.uni-tuebingen.de/~TMAD), and TOSS (http://astro.uni-tuebingen.de/~TOSS) services were constructed as part of the Tübingen project of the German Astrophysical

Virtual Observatory (GAVO, http://www.g-vo.org). This research has made use of NASA's Astrophysics Data System and the SIMBAD database, operated at CDS, Strasbourg, France.

References

Aggarwal, K. M., & Keenan, F. P. 2014, Phys. Scr., 89, 125404
Aggarwal, K. M., & Keenan, F. P. 2015, At. Data Nucl. Data Tables, 105, 9
Asplund, M., Grevesse, N., Sauval, A. J., & Scott, P. 2009, ARA&A, 47, 481
Biémont, E., Fischer, C. F., Godefroid, M. R., Palmeri, P., & Quinet, P. 2000, Phys. Rev. A, 62, 032512
Charro, E., & Martín, I. 1998, A&AS, 131, 523
Charro, E., & Martín, I. 2002, A&A, 395, 719
Charro, E., & Martín, I. 2005, Int. J. Quantum Chem., 104, 446
Chen, M. H., & Cheng, K. T. 2010, J. Phys. B, 43, 074019
Chou, H.-S., & Johnson, W. R. 1997, Phys. Rev. A, 56, 2424
Churilov, S. S., & Joshi, Y. N. 1995, Phys. Scr., 51, 196
Cowan, R. D. 1981, The theory of atomic structure and spectra (Berkeley, CA: University of California Press)
Crooker, A. M., & Joshi, Y. N. 1964, J. Opt. Soc. Am., 54, 553
Dreizler, S., & Werner, K. 1996, A&A, 314, 217
Dunne, P., & O'Sullivan, G. 1992, J. Phys. B, 25, L593
Fraga, S., Karwowski, J., & Saxena, K. M. S. 1976, Handbook of Atomic Data (Amsterdam: Elsevier)
Glowacki, L., & Migdalek, J. 2003, J. Phys. B At. Mol. Phys., 36, 3629
Głowacki, L., & Migdałek, J. 2009, Phys. Rev. A, 80, 042505
Grevesse, N., Scott, P., Asplund, M., & Sauval, A. J. 2015, A&A, 573, A27
Hoyer, D., Rauch, T., Werner, K., Kruk, J. W., & Quinet, P. 2017, A&A, 598, A135
Ivanova, E. P. 2011, Atomic Data and Nuclear Data Tables, 97, 1
Johnson, W. R., Kolb, D., & Huang, K.-N. 1983, Atomic Data and Nuclear Data Tables, 28, 333
Lemoine, M., Vidal-Madjar, A., Hébrard, G., et al. 2002, ApJS, 140, 67
Liu, Y., Hutton, R., Zou, Y., Andersson, M., & Brage, T. 2006, J. Phys. B, 39, 3147
McCook, G. P., & Sion, E. M. 1999a, ApJS, 121, 1
McCook, G. P., & Sion, E. M. 1999b, VizieR Online Data Catalog, 3210, 0
Migdalek, J., & Garmulewicz, M. 2000, J. Phys. B, 33, 1735
Müller-Ringat, E. 2013, Dissertation, University of Tübingen, Germany, http://nbn-resolving.de/urn:nbn:de:bsz:21-opus-67747
Preval, S. P., Barstow, M. A., Badnell, N. R., Hubeny, I., & Holberg, J. B. 2017, MNRAS, 465, 269
Quinet, P., Palmeri, P., Biémont, É., et al. 1999, MNRAS, 307, 934
Quinet, P., Palmeri, P., Biémont, É., et al. 2002, J. Alloys Comp., 344, 255
Rao, K. R., & Badami, J. S. 1931, Proc. Roy. Soc. Lond. A: Math., Phys. Eng. Sci., 131, 154
Rauch, T., & Deetjen, J. L. 2003, in Stellar Atmosphere Modeling, eds. I. Hubeny, D. Mihalas, & K. Werner, ASP Conf. Ser., 288, 103
Rauch, T., Werner, K., Biémont, É., Quinet, P., & Kruk, J. W. 2012, A&A, 546, A55
Rauch, T., Werner, K., Bohlin, R., & Kruk, J. W. 2013, A&A, 560, A106
Rauch, T., Werner, K., Quinet, P., & Kruk, J. W. 2014a, A&A, 564, A41
Rauch, T., Werner, K., Quinet, P., & Kruk, J. W. 2014b, A&A, 566, A10
Rauch, T., Werner, K., Quinet, P., & Kruk, J. W. 2015, A&A, 577, A6
Rauch, T., Quinet, P., Hoyer, D., et al. 2016a, A&A, 587, A39
Rauch, T., Quinet, P., Hoyer, D., et al. 2016b, A&A, 590, A128
Rauch, T., Gamrath, S., Quinet, P., et al. 2017, A&A, 599, A142
Ryabtsev, A. N., Churilov, S. S., & Kononov, É. Y. 2007, Opt. Spectrosc., 102, 354
Safronova, U. I., & Safronova, M. S. 2010, J. Phys. B, 43, 074025
Sansonetti, J. E. 2012, J. Phys. Chem. Ref. Data, 41, 013102
Scott, P., Asplund, M., Grevesse, N., Bergemann, M., & Sauval, A. J. 2015a, A&A, 573, A26
Scott, P., Grevesse, N., Asplund, M., et al. 2015b, A&A, 573, A25
Singh, A. K., Aggarwal, S., & Mohan, M. 2013, Phys. Scr., 88, 035301
Tauheed, A., Joshi, Y. N., & Pinnington, E. H. 1997, Phys. Scr., 56, 289
Werner, K., Deetjen, J. L., Dreizler, S., et al. 2003, in Stellar Atmosphere Modeling, eds. I. Hubeny, D. Mihalas, & K. Werner, ASP Conf. Ser., 288, 31
Werner, K., Dreizler, S., & Rauch, T. 2012a, Astrophysics Source Code Library [record ascl:1212.015]
Werner, K., Rauch, T., Ringat, E., & Kruk, J. W. 2012b, ApJ, 753, L7

Appendix A: Additional tables

Table A.1. Radial parameters (in cm^{-1}) adopted for the calculations in Se V.

Configuration	Parameter	HFR	Fitted	Ratio	Note[a]
		Even parity			
$4s^2$	E_{av}	7245	7181		
$4p^2$	E_{av}	220 372	224 026		
	F^2(4p, 4p)	59 154	53 762	0.909	
	α	0	457		
	ζ_{4p}	3088	3450	1.117	
4s4d	E_{av}	258 748	261 651		
	ζ_{4d}	182	226	1.243	
	G^2(4s, 4d)	37 575	24 976	0.665	
4s5d	E_{av}	383 599	385 096		
	ζ_{5d}	78	112	1.432	
	G^2(4s, 5d)	9177	5099	0.556	
4s5s	E_{av}	288 014	289 501		
	G^0(4s, 5s)	5161	4002	0.775	
4s6s	E_{av}	394 954	396 461		
	G^0(4s, 6s)	1704	1504	0.883	
		Odd parity			
4s4p	E_{av}	102 295	105 464		
	ζ_{4p}	3080	3488	1.133	
	G^1(4s, 4p)	78 837	67 261	0.853	
4s5p	E_{av}	326 870	329 516		
	ζ_{5p}	1011	1034	1.023	
	G^1(4s, 5p)	8447	7119	0.843	
4s4f	E_{av}	364 634	366 853		
	ζ_{4f}	2.5	2.5	1.000	F
	G^3(4s, 4f)	12 367	9673	0.782	
4p4d	E_{av}	369 549	374 676		
	ζ_{4p}	3207	3563	1.111	
	ζ_{4d}	188	188	1.000	F
	F^2(4p, 4d)	47 132	43 235	0.917	
	G^1(4p, 4d)	56 540	47 761	0.845	
	G^3(4p, 4d)	35 164	35 408	1.007	
4p5s	E_{av}	402 856	406 797		
	ζ_{4p}	3335	4134	1.240	
	G^1(4p, 5s)	7576	6819	0.900	F
4s4f–4p4d	R^1(4s, 4f; 4p, 4d)	44 911	41 100	0.915	R
	R^2(4s, 4f; 4p, 4d)	26 451	24 207	0.915	R

Notes. [(a)] F: fixed parameter value; Rn: ratios of these parameters have been fixed in the fitting process.

Table A.2. Radial parameters (in cm^{-1}) adopted for the calculations in Sr IV.

Configuration	Parameter	HFR	Fitted	Ratio	Note[a]
		Odd parity			
$4p^5$	E_{av}	17 382	17 802		
	ζ_{4p}	6193	6602	1.066	
$4p^4 5p$	E_{av}	297 016	284 223		
	F^2(4p, 4p)	72 698	59 785	0.822	
	α	0	−75		
	ζ_{4p}	6661	6788	1.019	
	ζ_{5p}	1144	1371	1.198	
	F^2(4p, 5p)	18 662	14 483	0.776	
	G^0(4p, 5p)	4032	3278	0.813	
	G^2(4p, 5p)	5306	3360	0.633	

Notes. [(a)] F: fixed parameter value; Rn: ratios of these parameters have been fixed in the fitting process.

Table A.2. continued.

Configuration	Parameter	HFR	Fitted	Ratio	Note[a]
$4p^4 6p$	E_{av}	376 793	363 483		
	$F^2(4p, 4p)$	72 878	60 207	0.826	
	α	0	−75		F
	ζ_{4p}	6690	6952	1.039	
	ζ_{6p}	481	481	1.000	F
	$F^2(4p, 6p)$	7047	6020	0.854	
	$G^0(4p, 6p)$	1379	1055	0.765	R1
	$G^2(4p, 6p)$	1925	1473	0.765	R1
$4p^4 4f$	E_{av}	361 378	349 638		
	$F^2(4p, 4p)$	72 733	65 254	0.897	
	α	0	−288		
	ζ_{4p}	6672	6946	1.041	
	ζ_{4f}	1.8	1.8	1.000	F
	$F^2(4p, 4f)$	16 152	16 436	1.018	
	$G^2(4p, 4f)$	7969	8546	1.072	R2
	$G^4(4p, 4f)$	5237	5616	1.072	R2
$4p^4 5f$	E_{av}	404 031	391 665		
	$F^2(4p,4p)$	72 850	65 565	0.900	F
	α	0	0		F
	ζ_{4p}	6687	6687	1.000	F
	ζ_{5f}	1.0	1.0	1.000	F
	$F^2(4p, 5f)$	7781	7003	0.900	F
	$G^2(4p, 5f)$	4809	4328	0.900	F
	$G^4(4p, 5f)$	3201	2881	0.900	F
$4p^4 6h$	E_{av}	429 580	417 003		
	$F^2(4p, 4p)$	73 002	59 206	0.811	
	α	0	0		F
	ζ_{4p}	6710	7010	1.045	
	ζ_{6h}	0.1	0.1	1.000	F
	$F^2(4p, 6h)$	955	859	0.900	F
	$G^4(4p, 6h)$	3.3	3.0	0.900	F
	$G^6(4p, 6h)$	2.4	2.2	0.900	F
$4s4p^5 4d$	E_{av}	406 219	389 470		
	ζ_{4p}	6396	6195	0.969	
	ζ_{4d}	347	347	1.000	F
	$F^2(4p, 4d)$	54 517	42 158	0.773	R3
	$G^1(4s, 4p)$	95 991	74 230	0.773	R3
	$G^2(4s, 4d)$	45 942	35 527	0.773	R3
	$G^1(4p, 4d)$	66 381	51 332	0.773	R3
	$G^3(4p, 4d)$	40 673	31 453	0.773	R3
$4p^4 4f$–$4s4p^5 4d$	$R^1(4s, 4f; 4p, 4d)$	33 789	25 846	0.765	R4
	$R^2(4s, 4f; 4p, 4d)$	17 934	13 718	0.765	R4
		Even parity			
$4s4p^6$	E_{av}	203 089	182 904		
$4p^4 4d$	E_{av}	229 165	216 300		
	$F^2(4p, 4p)$	71 296	66 892	0.938	
	α	0	−637		
	ζ_{4p}	6396	6821	1.066	
	ζ_{4d}	334	334	1.000	F
	$F^2(4p, 4d)$	53 739	44 659	0.831	
	$G^1(4p, 4d)$	65 079	51 977	0.799	
	$G^3(4p, 4d)$	39 867	33 775	0.847	

Table A.2. continued.

Configuration	Parameter	HFR	Fitted	Ratio	Note[a]
$4p^4 5d$	E_{av}	354 956	341 493		
	$F^2(4p, 4p)$	72 740	60 251	0.828	
	α	0	−60		
	ζ_{4p}	6654	6893	1.036	
	ζ_{5d}	92	92	1.000	F
	$F^2(4p, 5d)$	13 142	10 609	0.807	
	$G^1(4p, 5d)$	9350	5827	0.623	
	$G^3(4p, 5d)$	6407	4273	0.667	
$4p^4 6d$	E_{av}	402 278	388 769		
	$F^2(4p, 4p)$	72 887	56 086	0.769	
	α	0	147		
	ζ_{4p}	6686	6870	1.027	
	ζ_{6d}	43	43	1.000	F
	$F^2(4p, 6d)$	5594	4943	0.884	
	$G^1(4p, 6d)$	3610	2780	0.770	R5
	$G^3(4p, 6d)$	2568	1977	0.770	R5
$4p^4 5s$	E_{av}	256 289	243 230		
	$F^2(4p, 4p)$	72 284	68 498	0.948	
	α	0	−614		
	ζ_{4p}	6599	6882	1.043	
	$G^1(4p, 5s)$	6816	5379	0.789	
$4p^4 6s$	E_{av}	360 095	346 694		
	$F^2(4p, 4p)$	72 795	59 384	0.816	
	α	0	−53		
	ζ_{4p}	6674	6945	1.041	
	$G^1(4p, 6s)$	2042	1648	0.807	
$4p^4 7s$	E_{av}	404 294	391 199		
	$F^2(4p, 4p)$	72 908	62 746	0.861	
	α	0	−197		
	ζ_{4p}	6693	7217	1.078	
	$G^1(4p, 7s)$	923	831	0.900	F
$4p^4 5g$	E_{av}	407 514	395 098		
	$F^2(4p, 4p)$	72 989	59 801	0.819	
	α	0	0		F
	ζ_{4p}	6709	6709	1.000	F
	ζ_{5g}	0.4	0.4	1.000	F
	$F^2(4p, 5g)$	3168	2851	0.900	F
	$G^3(4p, 5g)$	178	160	0.900	F
	$G^5(4p, 5g)$	125	113	0.900	F
$4p^4 6g$	E_{av}	429 207	417 121		
	$F^2(4p, 4p)$	72 991	65 692	0.900	F
	α	0	0		F
	ζ_{4p}	6709	6709	1.000	F
	ζ_{6g}	0.2	0.2	1.000	F
	$F^2(4p, 6g)$	1820	1638	0.900	F
	$G^3(4p, 6g)$	167	150	0.900	F
	$G^5(4p, 6g)$	118	106	0.900	F
$4s4p^6$–$4p^4 4d$	$R^1(4p, 4p; 4s, 4d)$	76 477	58 890	0.770	

Table A.3. Radial parameters (in cm^{-1}) adopted for the calculations in Sr V.

Configuration	Parameter	HFR	Fitted	Ratio
	Even parity			
$4p^4$	E_{av}	26 722	27 025	
	$F^2(4p, 4p)$	73 003	66 387	0.909
	α	0	−116	
	ζ_{4p}	6711	7128	1.062
$4p^3 5p$	E_{av}	356 017	342 959	
	$F^2(4p, 4p)$	75 078	60 470	0.805
	α	0	−50	
	ζ_{4p}	7182	7453	1.038
	ζ_{5p}	1548	1903	1.230
	$F^2(4p, 5p)$	22 208	17 554	0.790
	$G^0(4p, 5p)$	4951	4056	0.819
	$G^2(4p, 5p)$	6500	3405	0.524
	Odd parity			
$4s4p^5$	E_{av}	208 535	192 965	
	ζ_{4p}	6714	6767	1.008
	$G^1(4s, 4p)$	97 914	82 694	0.845
$4p^3 4d$	E_{av}	256 391	244 342	
	$F^2(4p, 4p)$	73 706	66 981	0.909
	α	0	−579	
	ζ_{4p}	6889	7905	1.148
	ζ_{4d}	417	369	0.883
	$F^2(4p, 4d)$	58 919	50 755	0.861
	$G^1(4p, 4d)$	72 213	58 502	0.810
	$G^3(4p, 4d)$	44 593	38 327	0.859
$4p^3 5d$	E_{av}	426 470	412 624	
	$F^2(4p, 4p)$	75 124	61 062	0.813
	α	0	−53	
	ζ_{4p}	7175	7613	1.061
	ζ_{5d}	131	185	1.411
	$F^2(4p, 5d)$	16 331	11 882	0.728
	$G^1(4p, 5d)$	10 326	6815	0.660
	$G^3(4p, 5d)$	7360	3826	0.520
$4p^3 5s$	E_{av}	307 763	295 685	
	$F^2(4p, 4p)$	74 672	69 501	0.931
	α	0	−650	
	ζ_{4p}	7114	7661	1.077
	$G^1(4p, 5s)$	7725	5905	0.764
$4p^3 6s$	E_{av}	440 912	427 178	
	$F^2(4p, 4p)$	75 192	61 091	0.812
	α	0	−61	
	ζ_{4p}	7199	7573	1.052
	$G^1(4p, 6s)$	2418	1852	0.766
$4s4p^5$–$4p^3 4d$	$R^1(4p, 4p; 4s, 4d)$	82 213	63 348	0.771

Table A.4. Radial parameters (in cm^{-1}) adopted for the calculations in Sr VI.

Configuration	Parameter	HFR	Fitted	Ratio
	Odd parity			
$4p^3$	E_{av}	38 168	38 218	
	$F^2(4p, 4p)$	75 420	67 860	0.900
	α	0	−58	
	ζ_{4p}	7245	7847	1.083
	Even parity			
$4s4p^4$	E_{av}	215 385	207 203	
	$F^2(4p, 4p)$	75 398	65 586	0.870
	α	0	360	
	ζ_{4p}	7243	7548	1.042
	$G^1(4s, 4p)$	100 681	84 856	0.843
$4p^25s$	E_{av}	361 390	351 438	
	$F^2(4p, 4p)$	76 922	70 839	0.921
	α	0	−658	
	ζ_{4p}	7644	8279	1.083
	$G^1(4p, 5s)$	8511	6300	0.740

Table A.5. Radial parameters (in cm^{-1}) adopted for the calculations in Sr VII.

Configuration	Parameter	HFR	Fitted	Ratio
	Even parity			
$4p^2$	E_{av}	30 564	31 486	
	$F^2(4p, 4p)$	77 689	70 341	0.905
	α	0	−11	
	ζ_{4p}	7791	8364	1.073
	Odd parity			
$4s4p^3$	E_{av}	202 602	200 219	
	$F^2(4p, 4p)$	77 662	64 903	0.836
	α	0	401	
	ζ_{4p}	7783	8251	1.060
	$G^1(4s, 4p)$	103 310	89 586	0.867
4p5s	E_{av}	396 223	391 256	
	ζ_{4p}	8187	8710	1.064
	$G^1(4p, 5s)$	9207	6618	0.719

Table A.6. Radial parameters (in cm^{-1}) adopted for the calculations in Te VI.

Configuration	Parameter	HFR	Fitted	Ratio	
		Even parity			
$4d^{10}5s$	E_{av}	8200	8203		
$4d^{10}6s$	E_{av}	281 972	279 957		
$4d^{10}5d$	E_{av}	242 153	242 724		
	ζ_{5d}	544	651	1.198	
$4d^{9}5p^{2}$	E_{av}	514 322	508 542		
	$F^{2}(5p, 5p)$	54 096	55 453	1.025	
	ζ_{4d}	4672	4912	1.051	
	ζ_{5p}	7858	8936	1.137	
	$F^{2}(4d, 5p)$	36 688	31 239	0.851	
	$G^{1}(4d, 5p)$	11 365	10 095	0.888	R1
	$G^{3}(4d, 5p)$	10 856	9644	0.888	R1
		Odd parity			
$4d^{10}5p$	E_{av}	107 349	106 534		
	ζ_{5p}	7235	7936	1.097	
$4d^{10}6p$	E_{av}	320 537	318 496		
	ζ_{6p}	2768	2944	1.063	
$4d^{9}5s5p$	E_{av}	402 771	394 997		
	ζ_{4d}	4657	5044	1.083	
	ζ_{5p}	7882	8369	1.062	
	$F^{2}(4d, 5p)$	36 710	31 952	0.870	
	$G^{2}(4d, 5s)$	16 958	13 637	0.804	
	$G^{1}(4d, 5p)$	11 417	10 600	0.928	R2
	$G^{3}(4d, 5p)$	10 902	10 122	0.928	R2
	$G^{1}(5s, 5p)$	70 209	48 033	0.684	

Notes. [(a)] F: fixed parameter value; Rn: ratios of these parameters have been fixed in the fitting process.

Table A.7. Radial parameters (in cm^{-1}) adopted for the calculations in I VI.

Configuration	Parameter	HFR	Fitted	Ratio	
		Even parity			
$5s^2$	E_{av}	6244	6194		
$5p^2$	E_{av}	216 536	221 549		
	$F^2(5p, 5p)$	55 129	50 155	0.910	
	α	0	921		
	ζ_{5p}	8475	9377	1.106	
5s5d	E_{av}	252 535	256 150		
	ζ_{5d}	628	802	1.277	
	$G^2(5s, 5d)$	33 713	19 165	0.568	
5s6s	E_{av}	294 631	298 040		
	$G^0(5s, 6s)$	4762	3402	0.714	
5s7s	E_{av}	413 037	417 081		
	$G^0(5s, 7s)$	1619	1103	0.681	
		Odd parity			
5s5p	E_{av}	101 003	105 127		
	ζ_{5p}	8496	9361	1.102	
	$G^1(5s, 5p)$	71 600	55 279	0.772	
5s6p	E_{av}	336 195	341 270		
	ζ_{6p}	3039	3264	1.074	
	$G^1(5s, 6p)$	8024	6096	0.760	
5p5d	E_{av}	361 158	368 131		
	ζ_{5p}	8676	9398	1.083	
	ζ_{5d}	642	642	1.000	F
	$F^2(5p, 5d)$	45 177	37 226	0.824	
	$G^1(5p, 5d)$	52 465	40 477	0.772	R
	$G^3(5p, 5d)$	33 477	25 827	0.772	R
5p6s	E_{av}	406 984	413 299		
	ζ_{5p}	8954	9786	1.093	
	$G^1(5p, 6s)$	7259	7421	1.022	

Notes. [(a)] F: fixed parameter value; Rn: ratios of these parameters have been fixed in the fitting process.

Table A.8. Comparison between available experimental and calculated energy levels in Se V.

E_{exp} [a]	E_{calc} [b]	ΔE	J	Leading components (in %) in LS coupling[c]
				Even parity
0	0	0	0	97 $4s^2\ ^1S$
211 794	211 776	18	0	98 $4p^2\ ^3P$
213 203	213 206	−3	2	63 $4p^2\ ^1D$ + 20 $4p^2\ ^3P$ + 17 $4s4d\ ^1D$
214 091	214 117	−26	1	100 $4p^2\ ^3P$
218 615	218 604	11	2	80 $4p^2\ ^3P$ + 15 $4p^2\ ^1D$
248 787	248 787	0	0	94 $4p^2\ ^1S$
257 536	257 535	1	1	100 $4s4d\ ^3D$
257 750	257 751	−1	2	99 $4s4d\ ^3D$
258 082	258 082	0	3	99 $4s4d\ ^3D$
279 038	279 038	0	2	77 $4s4d\ ^1D$ + 21 $4p^2\ ^1D$
287 422	287 422	0	1	100 $4s5s\ ^3S$
295 381	295 381	0	0	99 $4s5s\ ^1S$
384 101	384 103	−2	1	100 $4s5d\ ^3D$
384 207	384 205	2	2	100 $4s5d\ ^3D$
384 376	384 377	−1	3	100 $4s5d\ ^3D$
386 684	386 684	0	2	98 $4s5d\ ^1D$
395 720	395 720	0	1	100 $4s6s\ ^3S$
398 817	398 817	0	0	100 $4s6s\ ^1S$
				Odd parity
89 749	89 754	−5	0	100 $4s4p\ ^3P$
91 350	91 342	8	1	99 $4s4p\ ^3P$
94 960	94 962	−2	2	100 $4s4p\ ^3P$
131 733	131 728	5	1	97 $4s4p\ ^1P$
326 298	326 290	8	0	99 $4s5p\ ^3P$
326 631	326 643	−12	1	94 $4s5p\ ^3P$ + 5 $4s5p\ ^1P$
327 843	327 838	5	2	99 $4s5p\ ^3P$
329 640	329 642	−2	1	91 $4s5p\ ^1P$ + 5 $4s5p\ ^3P$
351 880	351 691	189	2	66 $4p4d\ ^3F$ + 32 $4s4f\ ^3F$
353 241	352 999	242	3	62 $4p4d\ ^3F$ + 36 $4s4f\ ^3F$
355 112	354 758	354	4	56 $4p4d\ ^3F$ + 43 $4s4f\ ^3F$
358 148	358 319	−171	3	77 $4s4f\ ^1F$ + 21 $4p4d\ ^1F$
363 473	363 457	16	2	94 $4p4d\ ^1D$
372 695	372 550	145	2	45 $4s4f\ ^3F$ + 19 $4p4d\ ^3F$ + 18 $4p4d\ ^3D$
373 227	373 379	−152	3	60 $4s4f\ ^3F$ + 32 $4p4d\ ^3F$ + 7 $4p4d\ ^3D$
373 386	373 684	−298	1	65 $4p4d\ ^3D$ + 33 $4p4d\ ^3P$
373 700	373 883	−183	2	46 $4p4d\ ^3P$ + 20 $4s4f\ ^3F$ + 16 $4p4d\ ^3D$
374 294	374 707	−413	4	57 $4s4f\ ^3F$ + 43 $4p4d\ ^3F$
376 667	376 681	−14	0	98 $4p4d\ ^3P$
377 057	377 001	56	1	65 $4p4d\ ^3P$ + 33 $4p4d\ ^3D$
377 171	377 172	−1	3	92 $4p4d\ ^3D$
377 216	377 295	−79	2	64 $4p4d\ ^3D$ + 33 $4p4d\ ^3P$
399 060	399 388	−328	1	79 $4p4d\ ^1P$ + 9 $4p5s\ ^1P$
401 867	401 730	137	0	97 $4p5s\ ^3P$
402 722	402 847	−125	1	76 $4p5s\ ^3P$ + 10 $4p4d\ ^1P$ + 8 $4p5s\ ^1P$
404 273	403 620	653	3	65 $4p4d\ ^1F$ + 20 $4s4f\ ^1F$ + 12 $4s5f\ ^1F$
407 500	407 709	−209	2	94 $4p5s\ ^3P$ + 5 $4s6p\ ^3P$
408 693	408 321	372	1	43 $4p5s\ ^1P$ + 34 $4s6p\ ^1P$ + 14 $4p5s\ ^3P$

Notes. Energies are given in cm^{-1}. [a] From Churilov & Joshi (1995). [b] This work. [c] Only the first three components larger than 5% are given.

Table A.9. Comparison between available experimental and calculated energy levels in Sr IV.

E_{exp}[a]	E_{calc}[b]	ΔE	J	Leading components (in %) in LS coupling[c]
				Odd parity
0.00	0	0	1.5	97 $4p^5\ ^2P$
9727.90	9728	0	0.5	97 $4p^5\ ^2P$
267 529.26	267 364	165	1.5	68 $4p^4(^3P)5p\ ^4P$ + 8 $4p^4(^3P)5p\ ^4S$ + 7 $4p^4(^3P)5p\ ^2P$
267 537.32	267 389	148	2.5	79 $4p^4(^3P)5p\ ^4P$ + 16 $4p^4(^3P)5p\ ^4D$
270 350.30	270 269	81	0.5	54 $4p^4(^3P)5p\ ^4P$ + 19 $4p^4(^3P)5p\ ^2P$ + 14 $4p^4(^1D)5p\ ^2P$
271 249.46	271 591	−342	3.5	93 $4p^4(^3P)5p\ ^4D$ + 7 $4p^4(^1D)5p\ ^2F$
271 328.56	271 425	−96	2.5	65 $4p^4(^3P)5p\ ^2D$ + 20 $4p^4(^3P)5p\ ^4D$ + 7 $4p^4(^1D)5p\ ^2F$
276 054.66	275 902	153	0.5	39 $4p^4(^3P)5p\ ^4P$ + 27 $4p^4(^3P)5p\ ^2P$ + 15 $4p^4(^1D)5p\ ^2P$
276 159.16	276 134	25	1.5	27 $4p^4(^3P)5p\ ^2D$ + 25 $4p^4(^3P)5p\ ^2P$ + 24 $4p^4(^3P)5p\ ^4D$
277 913.84	278 103	−189	0.5	84 $4p^4(^3P)5p\ ^4D$ + 5 $4p^4(^1S)5p\ ^2P$ + 5 $4p^4(^3P)5p\ ^2S$
278 078.00	278 102	−24	1.5	58 $4p^4(^3P)5p\ ^4D$ + 29 $4p^4(^3P)5p\ ^2P$ + 9 $4p^4(^1D)5p\ ^2P$
279 165.72	279 218	−52	2.5	61 $4p^4(^3P)5p\ ^4D$ + 27 $4p^4(^3P)5p\ ^2D$ + 10 $4p^4(^3P)5p\ ^4P$
281 543.86	281 410	134	1.5	36 $4p^4(^3P)5p\ ^4S$ + 20 $4p^4(^3P)5p\ ^2D$ + 16 $4p^4(^3P)5p\ ^4P$
282 345.52	282 160	186	1.5	48 $4p^4(^3P)5p\ ^2D$ + 39 $4p^4(^3P)5p\ ^4S$ + 6 $4p^4(^3P)5p\ ^2P$
282 440.51	282 647	−206	0.5	74 $4p^4(^3P)5p\ ^2S$ + 14 $4p^4(^3P)5p\ ^2P$
288 655.13	288 839	−184	2.5	89 $4p^4(^1D)5p\ ^2F$ + 6 $4p^4(^3P)5p\ ^2D$
290 311.89	290 490	−178	3.5	92 $4p^4(^1D)5p\ ^2F$ + 7 $4p^4(^3P)5p\ ^4D$
292 454.67	292 480	−25	1.5	60 $4p^4(^1D)5p\ ^2P$ + 19 $4p^4(^1D)5p\ ^2D$ + 11 $4p^4(^3P)5p\ ^2p$
294 867.62	294 728	140	1.5	75 $4p^4(^1D)5p\ ^2D$ + 14 $4p^4(^3P)5p\ ^2P$ + 9 $4p^4(^1D)5p\ ^2P$
295 118.74	294 893	226	2.5	93 $4p^4(^1D)5p\ ^2D$
297 705.09	297 725	−20	0.5	64 $4p^4(^1D)5p\ ^2P$ + 33 $4p^4(^3P)5p\ ^2P$
314 666.82	314 745	−78	0.5	87 $4p^4(^1S)5p\ ^2P$ + 5 $4p^4(^3P)5p\ ^2P$
315 791.69	315 708	84	1.5	89 $4p^4(^1S)5p\ ^2P$
328 551.41	328 892	−341	4.5	70 $4p^4(^3P)4f\ ^4F$ + 17 $4s4p^54d\ ^4F$ + 6 $4p^4(^3P)4f\ ^4G$
328 908.67	329 133	−224	3.5	70 $4p^4(^3P)4f\ ^4F$ + 15 $4s4p^54d\ ^4F$
329 681.06	329 822	−141	2.5	66 $4p^4(^3P)4f\ ^4F$ + 13 $4s4p^54d\ ^4F$ + 9 $4p^4(^3P)4f\ ^4D$
330 811.44	330 921	−110	1.5	63 $4p^4(^3P)4f\ ^4F$ + 12 $4s4p^54d\ ^4F$ + 11 $4p^4(^3P)4f\ ^4D$
334 267.61	334 048	220	0.5	77 $4s4p^54d\ ^4P$ + 9 $4p^34d^2\ ^4P$ + 6 $4p^4(^3P)4f\ ^4D$
335 379.10	335 055	324	5.5	90 $4p^4(^3P)4f\ ^4G$ + 8 $4p^4(^1D)4f\ ^2H$
335 389.12	335 209	180	1.5	66 $4s4p^54d\ ^4P$ + 10 $4p^4(^3P)4f\ ^4D$ + 8 $4p^34d^2\ ^4P$
335 431.13	335 375	56	0.5	77 $4p^4(^3P)4f\ ^4D$ + 8 $4p^4(^1D)4f\ ^2P$ + 6 $4s4p^54d\ ^4P$
335 706.85	335 694	13	2.5	50 $4p^4(^3P)4f\ ^2F$ + 21 $4p^4(^3P)4f\ ^4D$ + 11 $4p^4(^3P)4f\ ^2D$
335 779.95	335 685	95	4.5	60 $4p^4(^3P)4f\ ^2G$ + 29 $4p^4(^3P)4f\ ^4G$ + 9 $4p^4(^1D)4f\ ^2H$
335 780.35	335 624	156	3.5	62 $4p^4(^3P)4f\ ^2F$ + 15 $4p^4(^3P)4f\ ^2G$ + 9 $4p^4(^3P)4f\ ^4G$
336 723.73	336 701	23	1.5	46 $4p^4(^3P)4f\ ^4D$ + 21 $4p^4(^3P)4f\ ^2D$ + 15 $4s4p^54d\ ^4P$
338 194.34	337 807	387	2.5	74 $4s4p^54d\ ^4P$ + 10 $4p^34d^2\ ^4P$
340 337.91	340 565	−227	1.5	48 $4p^4(^3P)4f\ ^2D$ + 16 $4p^4(^3P)4f\ ^4D$ + 14 $4p^4(^3P)4f\ ^4F$
340 973.05	340 984	−11	2.5	50 $4p^4(^3P)4f\ ^4D$ + 13 $4p^4(^3P)4f\ ^2F$ + 10 $4p^4(^3P)4f\ ^4F$
341 157.71	341 194	−36	4.5	56 $4p^4(^3P)4f\ ^4G$ + 27 $4p^4(^3P)4f\ ^2G$ + 8 $4s4p^54d\ ^4F$
341 420.62	341 412	9	3.5	44 $4p^4(^3P)4f\ ^4D$ + 33 $4p^4(^3P)4f\ ^4G$ + 6 $4s4p^54d\ ^4D$
343 266.68	343 045	222	3.5	46 $4p^4(^3P)4f\ ^4G$ + 26 $4p^4(^3P)4f\ ^4D$ + 19 $4p^4(^3P)4f\ ^2F$
343 520.46	343 128	392	2.5	79 $4p^4(^3P)4f\ ^4G$ + 8 $4p^4(^3P)4f\ ^2F$ + 6 $4p^4(^1S)4f\ ^2F$
344 417.51	344 350	68	3.5	79 $4p^4(^3P)4f\ ^2G$ + 12 $4p^4(^3P)4f\ ^2F$
345 236.33	345 460	−224	2.5	77 $4p^4(^3P)4f\ ^2D$ + 8 $4p^4(^3P)4f\ ^2F$
349 952.33	349 755	197	2.5	72 $4p^4(^3P)6p\ ^4P$ + 20 $4p^4(^3P)6p\ ^4D$
350 211.08	350 104	107	1.5	58 $4p^4(^3P)6p\ ^4P$ + 16 $4p^4(^3P)6p\ ^4S$ + 8 $4p^4(^3P)6p\ ^4D$
350 449.73	350 666	−216	4.5	55 $4s4p^54d\ ^4F$ + 22 $4p^4(^3P)4f\ ^4F$ + 9 $4p^34d^2\ ^4F$
350 715.04	351 031	−316	3.5	47 $4s4p^54d\ ^4F$ + 10 $4p^4(^3P)4f\ ^4F$ + 10 $4p^4(^1D)4f\ ^2F$
351 166.74	351 274	−107	2.5	34 $4p^4(^1D)4f\ ^2D$ + 30 $4p^4(^3P)6p\ ^2D$ + 11 $4s4p^54d\ ^2D$
351 443.45	351 583	−140	2.5	40 $4p^4(^3P)6p\ ^2D$ + 30 $4p^4(^1D)4f\ ^2D$ + 7 $4p^4(^3P)6p\ ^4D$
351 462.05	351 481	−19	3.5	83 $4p^4(^3P)6p\ ^4D$ + 6 $4s4p^54d\ ^4F$ + 6 $4p^4(^1D)6p\ ^2F$
351 735.29	351 721	14	0.5	23 $4p^4(^3P)6p\ ^2S$ + 22 $4p^4(^1D)4f\ ^2P$ + 21 $4p^4(^3P)6p\ ^4P$
352 075.62	351 978	98	1.5	61 $4p^4(^1D)4f\ ^2P$ + 21 $4p^4(^1D)4f\ ^2D$ + 6 $4p^4(^3P)4f\ ^4D$
352 433.02	352 726	−293	2.5	52 $4s4p^54d\ ^4F$ + 14 $4p^4(^3P)4f\ ^4F$ + 9 $4p^34d^2\ ^4F$

Notes. Energies are given in cm^{-1}. [(a)] From Sansonetti (2012). [(b)] This work. [(c)] Only the first three components larger than 5% are given.

Table A.9. continued.

E_{exp}[a]	E_{calc}[b]	ΔE	J	Leading components (in %) in LS coupling[c]
352 624.10	352 846	−222	1.5	38 $4p^4(^1D)4f\ ^2D$ + 21 $4p^4(^1D)4f\ ^2P$ + 15 $4p^4(^3P)4f\ ^2D$
353 156.17	352 847	309	4.5	88 $4p^4(^1D)4f\ ^2H$ + 7 $4p^4(^3P)4f\ ^2G$
353 192.24	352 883	309	5.5	89 $4p^4(^1D)4f\ ^2H$ + 8 $4p^4(^3P)4f\ ^4G$
353 899.14	353 996	−97	1.5	43 $4p^4(^3P)6p\ ^2P$ + 21 $4p^4(^3P)6p\ ^4S$ + 18 $4p^4(^3P)6p\ ^2D$
353 937.37	353 977	−40	3.5	51 $4p^4(^1D)4f\ ^2F$ + 26 $4s4p^54d\ ^2F$ + 7 $4p^4(^3P)4f\ ^4F$
354 435.30	354 632	−197	1.5	54 $4s4p^54d\ ^4F$ + 15 $4p^4(^3P)4f\ ^4F$ + 9 $4p^34d^2\ ^4F$
355 372.02	355 567	−195	2.5	62 $4p^4(^1D)4f\ ^2F$ + 14 $4s4p^54d\ ^2F$ + 7 $4p^4(^3P)4f\ ^2F$
357 530.83	357 698	−167	3.5	91 $4p^4(^1D)4f\ ^2G$
357 874.78	358 079	−204	4.5	90 $4p^4(^1D)4f\ ^2G$
358 151.51	358 073	79	0.5	67 $4p^4(^3P)6p\ ^4P$ + 19 $4p^4(^3P)6p\ ^2S$ + 10 $4p^4(^3P)6p\ ^2P$
359 197.56	359 242	−44	0.5	86 $4p^4(^3P)6p\ ^4D$ + 6 $4p^4(^1S)6p\ ^2P$
359 228.65	359 279	−50	1.5	73 $4p^4(^3P)6p\ ^4D$ + 13 $4p^4(^3P)6p\ ^2P$ + 7 $4p^4(^3P)6p\ ^4P$
359 420.70	359 343	78	2.5	61 $4p^4(^3P)6p\ ^4D$ + 20 $4p^4(^3P)6p\ ^2D$ + 17 $4p^4(^3P)6p\ ^4P$
360 344.74	360 559	−214	0.5	63 $4s4p^54d\ ^4D$ + 7 $4p^4(^3P)4f\ ^4D$ + 7 $4p^4(^3P)5f\ ^4D$
360 403.00	360 247	156	1.5	48 $4p^4(^3P)6p\ ^4S$ + 22 $4p^4(^3P)6p\ ^2D$ + 19 $4p^4(^3P)6p\ ^4P$
360 539.33	360 344	195	3.5	44 $4s4p^54d\ ^2F$ + 28 $4p^4(^1D)4f\ ^2F$
360 770.07	360 877	−107	1.5	53 $4p^4(^3P)6p\ ^2D$ + 25 $4p^4(^3P)6p\ ^2P$ + 7 $4p^4(^3P)6p\ ^4P$
361 194.32	361 363	−169	0.5	45 $4p^4(^3P)6p\ ^2P$ + 44 $4p^4(^3P)6p\ ^2S$
361 406.28	361 453	−47	1.5	60 $4s4p^54d\ ^4D$ + 8 $4p^4(^3P)4f\ ^4D$ + 6 $4s4p^54d\ ^4F$
361 478.30	361 498	−20	2.5	55 $4s4p^54d\ ^4D$ + 7 $4p^4(^3P)4f\ ^4D$ + 7 $4s4p^54d\ ^4F$
363 743.37	363 514	229	2.5	36 $4s4p^54d\ ^2F$ + 17 $4s4p^54d\ ^2D$ + 12 $4p^4(^1D)4f\ ^2F$
367 291.31	367 469	−178	1.5	55 $4s4p^54d\ ^2D$ + 17 $4p^4(^1D)4f\ ^2D$
368 412.00	368 034	378	2.5	38 $4s4p^54d\ ^2D$ + 22 $4s4p^54d\ ^2F$ + 10 $4p^4(^1D)4f\ ^2D$
370 570.27	370 644	−74	2.5	87 $4p^4(^1D)6p\ ^2F$
371 246.97	371 196	51	3.5	91 $4p^4(^1D)6p\ ^2F$ + 6 $4p^4(^3P)6p\ ^4D$
372 804.73	372 802	3	1.5	91 $4p^4(^1D)6p\ ^2D$ + 5 $4p^4(^3P)6p\ ^2P$
373 036.14	372 939	97	2.5	91 $4p^4(^1D)6p\ ^2D$
376 797.49	377 180	−383	2.5	31 $4p^4(^3P)5f\ ^2F$ + 21 $4p^4(^1S)4f\ ^2F$ + 10 $4p^4(^3P)5f\ ^4F$
376 898.93	376 783	116	3.5	49 $4p^4(^1S)4f\ ^2F$ + 20 $4p^4(^3P)5f\ ^2F$ + 5 $4p^4(^3P)5f\ ^4G$
377 521.69	377 951	−429	4.5	42 $4p^4(^3P)5f\ ^4F$ + 46 $4p^4(^3P)5f\ ^4G$
377 552.45	377 832	−280	5.5	92 $4p^4(^3P)5f\ ^4G$ + 6 $4p^4(^1D)5f\ ^2H$
377 766.96	378 204	−437	4.5	72 $4p^4(^3P)5f\ ^2G$ + 14 $4p^4(^3P)5f\ ^4F$
378 028.81	378 296	−267	3.5	44 $4p^4(^3P)5f\ ^4F$ + 16 $4p^4(^3P)5f\ ^4G$ + 16 $4p^4(^1S)4f\ ^2F$
378 524.75	378 495	30	2.5	54 $4p^4(^1S)4f\ ^2F$ + 11 $4p^4(^3P)5f\ ^4F$ + 8 $4p^4(^3P)5f\ ^2F$
379 962.16	378 865	1097	3.5	37 $4p^4(^3P)5f\ ^2F$ + 14 $4p^4(^3P)5f\ ^4F$ + 13 $4p^4(^3P)5f\ ^2G$
380 835.09	379 239	1596	2.5	34 $4p^4(^3P)5f\ ^4D$ + 30 $4p^4(^3P)5f\ ^4F$ + 15 $4p^4(^3P)5f\ ^2F$
405 022.76	405 019	4	4.5	38 $4p^4(^3P)6h\ ^4H$ + 25 $4p^4(^3P)6h\ ^2H$ + 15 $4p^4(^3P)6h\ ^2G$
405 024.04	405 020	4	5.5	47 $4p^4(^3P)6h\ ^4H$ + 21 $4p^4(^3P)6h\ ^4G$ + 16 $4p^4(^3P)6h\ ^2H$
405 025.99	405 027	−1	5.5	42 $4p^4(^3P)6h\ ^2H$ + 22 $4p^4(^3P)6h\ ^4I$ + 15 $4p^4(^3P)6h\ ^2I$
405 026.55	405 028	−1	6.5	56 $4p^4(^3P)6h\ ^4H$ + 27 $4p^4(^3P)6h\ ^4I$ + 11 $4p^4(^3P)6h\ ^2I$
405 086.10	405 082	4	3.5	39 $4p^4(^3P)6h\ ^4H$ + 32 $4p^4(^3P)6h\ ^4G$ + 22 $4p^4(^3P)6h\ ^2G$
405 087.28	405 082	5	4.5	40 $4p^4(^3P)6h\ ^4G$ + 24 $4p^4(^3P)6h\ ^2H$ + 15 $4p^4(^3P)6h\ ^4H$
405 139.33	405 153	−14	7.5	93 $4p^4(^3P)6h\ ^4I$ + 6 $4p^4(^1D)6h\ ^2K$
405 140.77	405 153	−12	6.5	67 $4p^4(^3P)6h\ ^2I$ + 27 $4p^4(^3P)6h\ ^4I$ + 6 $4p^4(^1D)6h\ ^2K$
405 180.62	405 179	2	3.5	55 $4p^4(^3P)6h\ ^2G$ + 39 $4p^4(^3P)6h\ ^4G$ + 7 $4p^4(^1D)6h\ ^2F$
405 182.67	405 177	6	2.5	92 $4p^4(^3P)6h\ ^4G$ + 7 $4p^4(^1D)6h\ ^2F$
413 358.39	413 362	−4	5.5	36 $4p^4(^3P)6h\ ^4I$ + 29 $4p^4(^3P)6h\ ^2H$ + 23 $4p^4(^3P)6h\ ^2I$
413 359.39	413 363	−4	6.5	43 $4p^4(^3P)6h\ ^4I$ + 40 $4p^4(^3P)6h\ ^4H$ + 17 $4p^4(^3P)6h\ ^2I$
413 480.05	413 481	−1	4.5	47 $4p^4(^3P)6h\ ^4I$ + 37 $4p^4(^3P)6h\ ^2G$ + 13 $4p^4(^3P)6h\ ^4G$
413 480.27	413 481	−1	5.5	51 $4p^4(^3P)6h\ ^4G$ + 29 $4p^4(^3P)6h\ ^2I$ + 18 $4p^4(^3P)6h\ ^4I$
413 807.07	413 791	16	4.5	18 $4p^4(^3P)6h\ ^2G$ + 38 $4p^4(^3P)6h\ ^4I$ + 17 $4p^4(^3P)6h\ ^4H$
425 272.55	425 281	−8	7.5	93 $4p^4(^1D)6h\ ^2K$ + 6 $4p^4(^3P)6h\ ^4I$
425 273.51	425 280	−6	6.5	93 $4p^4(^1D)6h\ ^2K$
425 399.44	425 384	15	3.5	93 $4p^4(^1D)6h\ ^2G$
425 399.98	425 384	16	4.5	93 $4p^4(^1D)6h\ ^2G$
425 519.55	425 530	−10	5.5	94 $4p^4(^1D)6h\ ^2I$

Table A.9. continued.

E_{exp}[a]	E_{calc}[b]	ΔE	J	Leading components (in %) in LS coupling[c]
425 520.26	425 530	−10	6.5	94 $4p^4(^1D)6h\ ^2I$
425 530.88	425 532	−1	5.5	93 $4p^4(^1D)6h\ ^2H$
425 532.42	425 531	1	4.5	94 $4p^4(^1D)6h\ ^2H$
				Even parity
150 504.10	150 530	−26	0.5	73 $4s4p^6\ ^2S$ + 26 $4p^4(^1D)4d\ ^2S$
187 160.33	187 072	88	3.5	93 $4p^4(^3P)4d\ ^4D$
187 200.74	187 180	21	2.5	91 $4p^4(^3P)4d\ ^4D$
188 024.11	188 082	−58	1.5	90 $4p^4(^3P)4d\ ^4D$
189 119.64	189 294	−174	0.5	90 $4p^4(^3P)4d\ ^4D$
197 060.03	196 254	806	4.5	92 $4p^4(^3P)4d\ ^4F$ + 8 $4p^4(^1D)4d\ ^2G$
200 340.03	199 760	580	3.5	79 $4p^4(^3P)4d\ ^4F$ + 10 $4p^4(^3P)4d\ ^2F$ + 8 $4p^4(^1D)4d\ ^2G$
200 529.25	201 801	−1272	0.5	44 $4p^4(^1D)4d\ ^2P$ + 40 $4p^4(^3P)4d\ ^2P$ + 9 $4p^4(^3P)4d\ ^4D$
203 344.42	202 748	596	2.5	94 $4p^4(^3P)4d\ ^4F$
204 179.71	203 710	470	1.5	90 $4p^4(^3P)4d\ ^4F$ + 5 $4p^4(^1S)4d\ ^2D$
204 743.50	204 854	−111	0.5	91 $4p^4(^3P)4d\ ^4P$
204 808.95	205 235	−426	1.5	60 $4p^4(^3P)4d\ ^4P$ + 19 $4p^4(^1D)4d\ ^2P$ + 10 $4p^4(^3P)4d\ ^2P$
206 524.12	206 915	−391	1.5	40 $4p^4(^1D)4d\ ^2D$ + 27 $4p^4(^3P)4d\ ^2D$ + 11 $4p^4(^3P)4d\ ^2P$
207 478.23	207 601	−123	3.5	54 $4p^4(^3P)4d\ ^2F$ + 20 $4p^4(^1D)4d\ ^2G$ + 14 $4p^4(^3P)4d\ ^4F$
208 937.80	208 997	−59	2.5	84 $4p^4(^3P)4d\ ^4P$
209 211.07	209 873	−662	1.5	32 $4p^4(^3P)4d\ ^4P$ + 25 $4p^4(^1D)4d\ ^2P$ + 23 $4p^4(^3P)4d\ ^2P$
211 973.07	212 246	−273	2.5	38 $4p^4(^1D)4d\ ^2D$ + 24 $4p^4(^3P)4d\ ^2D$ + 18 $4p^4(^3P)4d\ ^2F$
214 946.01	215 491	−545	2.5	63 $4p^4(^3P)4d\ ^2F$ + 16 $4p^4(^1D)4d\ ^2F$ + 14 $4p^4(^1D)4d\ ^2D$
215 187.68	214 351	837	4.5	92 $4p^4(^1D)4d\ ^2G$ + 8 $4p^4(^3P)4d\ ^4F$
215 188.35	214 668	520	3.5	71 $4p^4(^1D)4d\ ^2G$ + 20 $4p^4(^3P)4d\ ^2F$ + 7 $4p^4(^1D)4d\ ^2F$
225 871.18	225 862	9	2.5	82 $4p^4(^1D)4d\ ^2F$ + 10 $4p^4(^3P)4d\ ^2F$ + 6 $4p^4(^1D)4d\ ^2D$
228 097.73	228 172	−74	3.5	83 $4p^4(^1D)4d\ ^2F$ + 15 $4p^4(^3P)4d\ ^2F$
228 654.17	228 689	−35	2.5	92 $4p^4(^3P)5s\ ^4P$
232 210.43	232 159	51	1.5	47 $4p^4(^3P)5s\ ^4P$ + 45 $4p^4(^3P)5s\ ^2P$ + 6 $4p^4(^1D)5s\ ^2D$
236 924.66	236 911	14	0.5	93 $4p^4(^3P)5s\ ^4P$
238 217.98	238 212	6	1.5	51 $4p^4(^3P)5s\ ^4P$ + 46 $4p^4(^3P)5s\ ^2P$
242 092.84	242 123	−30	0.5	95 $4p^4(^3P)5s\ ^2P$
242 171.57	242 100	72	1.5	60 $4p^4(^1S)4d\ ^2D$ + 26 $4p^4(^1D)4d\ ^2D$
245 734.92	245 693	42	2.5	66 $4p^4(^1S)4d\ ^2D$ + 19 $4p^4(^1D)4d\ ^2D$
250 046.76	250 115	−68	2.5	86 $4p^4(^1D)5s\ ^2D$ + 6 $4p^4(^3P)4d\ ^2D$ + 5 $4p^4(^3P)5s\ ^4P$
250 503.65	250 424	80	1.5	87 $4p^4(^1D)5s\ ^2D$ + 8 $4p^4(^3P)5s\ ^2P$
252 385.97	252 298	88	1.5	44 $4p^4(^3P)4d\ ^2P$ + 35 $4p^4(^1D)4d\ ^2P$ + 8 $4p^4(^1D)4d\ ^2D$
253 231.79	253 243	−11	0.5	44 $4p^4(^1D)4d\ ^2S$ + 17 $4p^4(^1D)4d\ ^2P$ + 16 $4p^4(^3P)4d\ ^2P$
254 820.96	254 940	−119	2.5	51 $4p^4(^3P)4d\ ^2D$ + 19 $4p^4(^1S)4d\ ^2D$ + 18 $4p^4(^1D)4d\ ^2D$
257 344.99	257 053	292	0.5	33 $4p^4(^3P)4d\ ^2P$ + 30 $4p^4(^1D)4d\ ^2P$ + 23 $4p^4(^1D)4d\ ^2S$
264 181.57	264 199	−17	1.5	48 $4p^4(^3P)4d\ ^2D$ + 23 $4p^4(^1S)4d\ ^2D$ + 12 $4p^4(^1D)4d\ ^2D$
274 687.97	274 692	−4	0.5	85 $4p^4(^1S)5s\ ^2S$
327 166.57	327 138	29	3.5	76 $4p^4(^3P)5d\ ^4D$ + 17 $4p^4(^3P)5d\ ^4F$
327 296.31	327 263	33	2.5	73 $4p^4(^3P)5d\ ^4D$ + 11 $4p^4(^3P)5d\ ^4P$ + 9 $4p^4(^3P)5d\ ^4F$
327 865.89	327 824	42	1.5	62 $4p^4(^3P)5d\ ^4D$ + 23 $4p^4(^3P)5d\ ^4P$
328 733.88	328 723	11	0.5	48 $4p^4(^3P)5d\ ^4D$ + 29 $4p^4(^3P)5d\ ^4P$ + 13 $4p^4(^3P)5d\ ^2P$
329 068.54	329 092	−23	4.5	93 $4p^4(^3P)5d\ ^4F$ + 7 $4p^4(^1D)5d\ ^2G$
329 973.93	329 929	45	3.5	65 $4p^4(^3P)5d\ ^2F$ + 26 $4p^4(^3P)5d\ ^4F$ + 8 $4p^4(^1D)5d\ ^2G$
331 574.88	331 618	−43	0.5	59 $4p^4(^3P)5d\ ^4P$ + 24 $4p^4(^3P)5d\ ^2P$ + 8 $4p^4(^3P)5d\ ^4D$
333 030.58	333 041	−10	1.5	48 $4p^4(^3P)5d\ ^4P$ + 23 $4p^4(^3P)5d\ ^2D$ + 11 $4p^4(^3P)5d\ ^2P$
333 195.98	333 242	−46	2.5	29 $4p^4(^3P)5d\ ^2F$ + 24 $4p^4(^3P)5d\ ^2D$ + 21 $4p^4(^3P)5d\ ^4F$
334 143.89	334 146	−2	2.5	93 $4p^4(^3P)6s\ ^4P$ + 6 $4p^4(^1D)6s\ ^2D$
335 436.88	335 436	1	1.5	70 $4p^4(^3P)6s\ ^2P$ + 22 $4p^4(^3P)6s\ ^4P$ + 7 $4p^4(^1D)6s\ ^2D$
336 333.74	336 441	−107	0.5	43 $4p^4(^3P)5d\ ^4D$ + 39 $4p^4(^3P)5d\ ^2P$ + 10 $4p^4(^1D)5d\ ^2P$
336 898.26	336 807	91	3.5	53 $4p^4(^3P)5d\ ^4F$ + 25 $4p^4(^3P)5d\ ^2F$ + 20 $4p^4(^3P)5d\ ^4D$
337 047.44	337 088	−41	1.5	68 $4p^4(^3P)5d\ ^4F$ + 16 $4p^4(^3P)5d\ ^4D$ + 7 $4p^4(^3P)5d\ ^4P$
337 151.32	337 104	47	2.5	50 $4p^4(^3P)5d\ ^4F$ + 24 $4p^4(^3P)5d\ ^4P$ + 16 $4p^4(^3P)5d\ ^4D$

Table A.9. continued.

E_{exp} [a]	E_{calc} [b]	ΔE	J	Leading components (in %) in LS coupling[c]
337 963.83	337 983	−19	1.5	24 $4p^4(^3P)5d\ ^2D$ + 21 $4p^4(^3P)5d\ ^4F$ + 16 $4p^4(^3P)5d\ ^4D$
338 581.20	338 353	228	2.5	40 $4p^4(^3P)5d\ ^2F$ + 39 $4p^4(^3P)5d\ ^4P$ + 15 $4p^4(^3P)5d\ ^4F$
341 045.43	341 124	−79	2.5	54 $4p^4(^3P)5d\ ^2D$ + 27 $4p^4(^3P)5d\ ^2F$
341 216.97	341 431	−214	1.5	57 $4p^4(^3P)5d\ ^2P$ + 21 $4p^4(^3P)5d\ ^2D$ + 10 $4p^4(^1D)5d\ ^2P$
342 636.27	342 639	−3	0.5	93 $4p^4(^3P)6s\ ^4P$
342 700.06	342 694	6	1.5	75 $4p^4(^3P)6s\ ^4P$ + 23 $4p^4(^3P)6s\ ^2P$
344 195.86	344 195	1	0.5	94 $4p^4(^3P)6s\ ^2P$
348 103.87	348 175	−71	3.5	92 $4p^4(^1D)5d\ ^2G$ + 6 $4p^4(^3P)5d\ ^2F$
348 308.67	348 316	−7	4.5	93 $4p^4(^1D)5d\ ^2G$ + 7 $4p^4(^3P)5d\ ^4F$
350 510.38	350 515	−5	2.5	52 $4p^4(^1D)5d\ ^2D$ + 43 $4p^4(^1D)5d\ ^2F$
350 670.46	350 835	−165	0.5	74 $4p^4(^1D)5d\ ^2S$ + 16 $4p^4(^1D)5d\ ^2P$ + 6 $4p^4(^3P)5d\ ^4P$
350 832.42	350 515	317	1.5	81 $4p^4(^1D)5d\ ^2P$ + 7 $4p^4(^3P)5d\ ^2P$
351 385.40	351 308	77	3.5	94 $4p^4(^1D)5d\ ^2F$
351 726.93	351 804	−77	2.5	49 $4p^4(^1D)5d\ ^2F$ + 36 $4p^4(^1D)5d\ ^2D$ + 7 $4p^4(^3P)5d\ ^2D$
353 148.62	352 986	163	0.5	59 $4p^4(^1D)5d\ ^2P$ + 19 $4p^4(^3P)5d\ ^2P$ + 16 $4p^4(^1D)5d\ ^2S$
353 264.68	353 476	−211	1.5	69 $4p^4(^1D)5d\ ^2D$ + 16 $4p^4(^3P)5d\ ^2D$ + 7 $4p^4(^1D)6s\ ^2D$
354 841.85	354 801	41	2.5	92 $4p^4(^1D)6s\ ^2D$ + 6 $4p^4(^3P)6s\ ^4P$
354 937.05	354 964	−27	1.5	85 $4p^4(^1D)6s\ ^2D$ + 6 $4p^4(^1D)5d\ ^2D$ + 5 $4p^4(^3P)6s\ ^2P$
373 326.84	373 323	4	2.5	88 $4p^4(^1S)5d\ ^2D$
373 710.50	373 687	24	1.5	83 $4p^4(^1S)5d\ ^2D$ + 5 $4p^4(^3P)6d\ ^2D$
376 210.74	376 083	128	3.5	69 $4p^4(^3P)6d\ ^4D$ + 22 $4p^4(^3P)6d\ ^4F$ + 5 $4p^4(^1D)6d\ ^2F$
376 297.31	376 165	132	2.5	65 $4p^4(^3P)6d\ ^4D$ + 16 $4p^4(^3P)6d\ ^4P$ + 12 $4p^4(^3P)6d\ ^4F$
376 503.06	376 480	23	1.5	49 $4p^4(^3P)6d\ ^4D$ + 36 $4p^4(^3P)6d\ ^4P$
377 002.29	376 936	66	4.5	93 $4p^4(^3P)6d\ ^4F$ + 7 $4p^4(^1D)6d\ ^2G$
377 030.29	376 930	100	0.5	54 $4p^4(^3P)6d\ ^4P$ + 28 $4p^4(^3P)6d\ ^4D$ + 10 $4p^4(^3P)6d\ ^2P$
377 348.64	377 348	1	3.5	70 $4p^4(^3P)6d\ ^2F$ + 22 $4p^4(^3P)6d\ ^4F$ + 7 $4p^4(^1D)6d\ ^2G$
378 221.92	378 221	1	0.5	87 $4p^4(^1S)6s\ ^2S$ + 5 $4p^4(^3P)6s\ ^4P$
378 474.25	378 520	−46	0.5	44 $4p^4(^3P)6d\ ^2P$ + 31 $4p^4(^3P)6d\ ^4P$ + 11 $4p^4(^3P)6d\ ^4D$
378 892.59	378 645	248	2.5	93 $4p^4(^3P)7s\ ^4P$ + 6 $4p^4(^1D)7s\ ^2D$
378 914.97	379 241	−326	1.5	59 $4p^4(^3P)7s\ ^2P$ + 14 $4p^4(^3P)7s\ ^4P$ + 6 $4p^4(^3P)6d\ ^4P$
379 066.96	379 564	−497	2.5	36 $4p^4(^3P)6d\ ^2D$ + 26 $4p^4(^3P)6d\ ^2F$ + 17 $4p^4(^3P)6d\ ^4P$
379 680.74	379 624	57	1.5	25 $4p^4(^3P)6d\ ^4P$ + 21 $4p^4(^3P)6d\ ^2D$ + 18 $4p^4(^3P)6d\ ^2P$
382 891.60	383 028	−136	5.5	62 $4p^4(^3P)5g\ ^4G$ + 24 $4p^4(^3P)5g\ ^4H$ + 9 $4p^4(^3P)5g\ ^2H$
382 897.81	383 019	−121	4.5	65 $4p^4(^3P)5g\ ^4G$ + 15 $4p^4(^3P)5g\ ^4H$ + 15 $4p^4(^3P)5g\ ^4F$
382 914.84	383 040	−125	3.5	45 $4p^4(^3P)5g\ ^4G$ + 21 $4p^4(^3P)5g\ ^2G$ + 11 $4p^4(^3P)5g\ ^2F$
382 932.42	383 094	−162	4.5	62 $4p^4(^3P)5g\ ^2G$ + 18 $4p^4(^3P)5g\ ^2H$ + 8 $4p^4(^3P)5g\ ^4H$
383 134.13	383 260	−126	2.5	41 $4p^4(^3P)5g\ ^4G$ + 31 $4p^4(^3P)5g\ ^4F$ + 21 $4p^4(^3P)5g\ ^2F$
383 151.49	383 294	−143	3.5	35 $4p^4(^3P)5g\ ^4F$ + 30 $4p^4(^3P)5g\ ^2G$ + 17 $4p^4(^3P)5g\ ^2F$
383 277.00	383 513	−236	6.5	94 $4p^4(^3P)5g\ ^4H$ + 6 $4p^4(^1D)5g\ ^2I$
383 286.02	383 528	−242	5.5	68 $4p^4(^3P)5g\ ^2H$ + 26 $4p^4(^3P)5g\ ^4H$ + 6 $4p^4(^1D)5g\ ^2I$
383 451.04	383 604	−153	1.5	92 $4p^4(^3P)5g\ ^4F$ + 7 $4p^4(^1D)5g\ ^2D$
383 457.36	383 628	−171	2.5	53 $4p^4(^3P)5g\ ^2F$ + 39 $4p^4(^3P)5g\ ^4F$ + 7 $4p^4(^1D)5g\ ^2D$
384 695.31	384 665	30	0.5	60 $4p^4(^3P)6d\ ^4D$ + 29 $4p^4(^3P)6d\ ^2P$ + 8 $4p^4(^3P)6d\ ^4P$
384 999.12	384 800	199	3.5	52 $4p^4(^3P)6d\ ^4F$ + 26 $4p^4(^3P)6d\ ^4D$ + 21 $4p^4(^3P)6d\ ^2F$
385 158.09	384 944	214	1.5	50 $4p^4(^3P)6d\ ^4F$ + 28 $4p^4(^3P)6d\ ^4D$ + 11 $4p^4(^3P)6d\ ^4P$
385 191.43	384 913	278	2.5	46 $4p^4(^3P)6d\ ^4F$ + 24 $4p^4(^3P)6d\ ^4D$ + 21 $4p^4(^3P)6d\ ^4P$
385 489.76	385 471	19	1.5	36 $4p^4(^3P)6d\ ^4F$ + 16 $4p^4(^3P)6d\ ^4P$ + 14 $4p^4(^3P)6d\ ^2D$
385 744.98	385 547	198	2.5	36 $4p^4(^3P)6d\ ^2F$ + 35 $4p^4(^3P)6d\ ^4P$ + 23 $4p^4(^3P)6d\ ^4F$
386 725.54	387 102	−376	2.5	47 $4p^4(^3P)6d\ ^2D$ + 34 $4p^4(^3P)6d\ ^2F$ + 7 $4p^4(^3P)6d\ ^4P$
387 321.32	387 352	−31	1.5	80 $4p^4(^3P)7s\ ^4P$ + 19 $4p^4(^3P)7s\ ^2P$
387 472.75	387 925	−452	1.5	52 $4p^4(^3P)6d\ ^2P$ + 35 $4p^4(^3P)6d\ ^2D$
387 557.60	387 491	67	0.5	86 $4p^4(^3P)7s\ ^4P$ + 11 $4p^4(^3P)7s\ ^2P$
388 284.04	388 319	−35	0.5	86 $4p^4(^3P)7s\ ^2P$ + 8 $4p^4(^3P)7s\ ^4P$ + 5 $4p^4(^1S)7s\ ^2S$
391 242.82	390 968	275	2.5	56 $4p^4(^3P)5g\ ^4G$ + 24 $4p^4(^3P)5g\ ^4F$ + 19 $4p^4(^3P)5g\ ^2F$
391 257.50	390 996	262	3.5	34 $4p^4(^3P)5g\ ^4F$ + 32 $4p^4(^3P)5g\ ^2G$ + 25 $4p^4(^3P)5g\ ^4G$
391 323.38	391 106	217	5.5	47 $4p^4(^3P)5g\ ^4H$ + 35 $4p^4(^3P)5g\ ^4G$ + 18 $4p^4(^3P)5g\ ^2H$
391 336.49	391 131	205	4.5	41 $4p^4(^3P)5g\ ^4H$ + 25 $4p^4(^3P)5g\ ^2G$ + 24 $4p^4(^3P)5g\ ^2H$

Table A.9. continued.

E_{exp} [a]	E_{calc} [b]	ΔE	J	Leading components (in %) in LS coupling[c]
391 709.40	391 501	208	4.5	57 $4p^4(^3P)5g\ ^4F$ + 23 $4p^4(^3P)5g\ ^2H$ + 15 $4p^4(^3P)5g\ ^4H$
391 711.14	391 515	196	3.5	45 $4p^4(^3P)5g\ ^4H$ + 40 $4p^4(^3P)5g\ ^2F$ + 12 $4p^4(^3P)5g\ ^4F$
391 854.19	391 765	89	4.5	31 $4p^4(^3P)5g\ ^2H$ + 19 $4p^4(^3P)5g\ ^4F$ + 18 $4p^4(^3P)5g\ ^4H$
391 856.50	391 763	94	3.5	42 $4p^4(^3P)5g\ ^4H$ + 19 $4p^4(^3P)5g\ ^2F$ + 14 $4p^4(^3P)5g\ ^4G$
396 691.71	396 442	250	3.5	92 $4p^4(^1D)6d\ ^2G$ + 5 $4p^4(^3P)6d\ ^2F$
396 805.69	396 512	294	4.5	93 $4p^4(^1D)6d\ ^2G$ + 7 $4p^4(^3P)6d\ ^4F$
397 204.00	397 235	−31	1.5	91 $4p^4(^1D)6d\ ^2P$
397 314.00	397 084	230	0.5	83 $4p^4(^1D)6d\ ^2S$ + 10 $4p^4(^1D)6d\ ^2P$ + 6 $4p^4(^3P)6d\ ^4P$
397 631.75	397 512	120	2.5	54 $4p^4(^1D)6d\ ^2D$ + 41 $4p^4(^1D)6d\ ^2F$
397 965.00	398 529	−564	0.5	76 $4p^4(^1D)6d\ ^2P$ + 12 $4p^4(^3P)6d\ ^2P$ + 9 $4p^4(^1D)6d\ ^2S$
398 073.63	398 104	−30	2.5	52 $4p^4(^1D)6d\ ^2F$ + 39 $4p^4(^1D)6d\ ^2D$
398 091.68	397 868	224	3.5	94 $4p^4(^1D)6d\ ^2F$
398 299.95	398 893	−593	1.5	83 $4p^4(^1D)6d\ ^2D$ + 9 $4p^4(^3P)6d\ ^2D$
399 522.24	399 494	28	2.5	93 $4p^4(^1D)7s\ ^2D$ + 6 $4p^4(^3P)7s\ ^4P$
399 560.55	399 565	−4	1.5	89 $4p^4(^1D)7s\ ^2D$ + 6 $4p^4(^3P)7s\ ^2P$
403 039.04	403 057	−18	6.5	93 $4p^4(^1D)5g\ ^2I$ + 6 $4p^4(^3P)5g\ ^4H$
403 040.00	403 056	−16	5.5	93 $4p^4(^1D)5g\ ^2I$
403 387.96	403 291	97	3.5	94 $4p^4(^1D)5g\ ^2F$
403 396.12	403 305	91	2.5	94 $4p^4(^1D)5g\ ^2F$
403 806.14	403 809	−3	4.5	92 $4p^4(^1D)5g\ ^2G$
403 815.98	403 824	−8	3.5	93 $4p^4(^1D)5g\ ^2G$
403 863.95	403 893	−29	4.5	92 $4p^4(^1D)5g\ ^2H$
403 864.66	403 894	−29	5.5	92 $4p^4(^1D)5g\ ^2H$
404 652.67	404 593	60	5.5	58 $4p^4(^3P)6g\ ^4G$ + 25 $4p^4(^3P)6g\ ^4H$ + 9 $4p^4(^3P)6g\ ^2H$
404 657.76	404 651	7	4.5	59 $4p^4(^3P)6g\ ^2G$ + 19 $4p^4(^3P)6g\ ^2H$ + 8 $4p^4(^3P)6g\ ^4H$
404 681.82	404 598	84	3.5	45 $4p^4(^3P)6g\ ^4G$ + 17 $4p^4(^3P)6g\ ^2G$ + 12 $4p^4(^3P)6g\ ^4F$
404 690.21	404 586	104	4.5	61 $4p^4(^3P)6g\ ^4G$ + 16 $4p^4(^3P)6g\ ^4H$ + 15 $4p^4(^3P)6g\ ^4F$
404 803.93	404 745	59	3.5	35 $4p^4(^3P)6g\ ^4F$ + 32 $4p^4(^3P)6g\ ^2G$ + 20 $4p^4(^3P)6g\ ^2F$
404 860.73	404 862	−1	6.5	94 $4p^4(^3P)6g\ ^4H$ + 5 $4p^4(^1D)6g\ ^2I$
404 867.75	404 877	−9	5.5	69 $4p^4(^3P)6g\ ^2H$ + 26 $4p^4(^3P)6g\ ^4H$ + 5 $4p^4(^1D)6g\ ^2I$
404 970.53	404 913	58	1.5	94 $4p^4(^3P)6g\ ^4F$ + 5 $4p^4(^1D)6g\ ^2D$
404 981.69	404 943	39	2.5	56 $4p^4(^3P)6g\ ^2F$ + 38 $4p^4(^3P)6g\ ^4F$ + 5 $4p^4(^1D)6g\ ^2D$

Table A.10. Comparison between available experimental and calculated energy levels in Sr V.

E_{exp} [a]	E_{calc} [b]	ΔE	J	Leading components (in %) in LS coupling[c]
				Even parity
0.00	−15	15	2	91 $4p^4\ ^3P$ + 6 $4p^4\ ^1D$
8307.88	8276	32	1	97 $4p^4\ ^3P$
8718.47	8768	−50	0	89 $4p^4\ ^3P$ + 8 $4p^4\ ^1S$
20 310.51	20 311	0	2	91 $4p^4\ ^1D$ + 6 $4p^4\ ^3P$
44 050.41	44 048	2	0	88 $4p^4\ ^1S$ + 8 $4p^4\ ^3P$
313 726.94	313 649	78	1	89 $4p^3(^4S)5p\ ^5P$
314 143.18	314 071	72	2	82 $4p^3(^4S)5p\ ^5P$ + 10 $4p^3(^4S)5p\ ^3P$
316 119.90	316 246	−126	3	94 $4p^3(^4S)5p\ ^5P$
319 834.74	319 802	33	1	71 $4p^3(^4S)5p\ ^3P$ + 8 $4p^3(^2D)5p\ ^3P$ + 6 $4p^3(^4S)5p\ ^5P$
321 239.05	321 359	−120	2	75 $4p^3(^4S)5p\ ^3P$ + 14 $4p^3(^4S)5p\ ^5P$ + 7 $4p^3(^2D)5p\ ^3P$
321 640.81	321 575	66	0	88 $4p^3(^4S)5p\ ^3P$ + 5 $4p^3(^2D)5p\ ^3P$ + 5 $4p^3(^2P)5p\ ^3P$
331 198.24	330 927	271	1	38 $4p^3(^2D)5p\ ^3D$ + 35 $4p^3(^2D)5p\ ^1P$ + 9 $4p^3(^2P)5p\ ^1P$
334 364.87	334 248	117	2	44 $4p^3(^2D)5p\ ^3D$ + 38 $4p^3(^2D)5p\ ^3F$ + 10 $4p^3(^2P)5p\ ^3D$
336 623.27	336 638	−15	3	57 $4p^3(^2D)5p\ ^3F$ + 33 $4p^3(^2D)5p\ ^3D$ + 8 $4p^3(^2P)5p\ ^3D$
336 694.99	336 796	−101	2	46 $4p^3(^2D)5p\ ^3F$ + 41 $4p^3(^2D)5p\ ^3D$ + 6 $4p^3(^2P)5p\ ^1D$
337 454.30	337 268	186	1	43 $4p^3(^2D)5p\ ^1P$ + 43 $4p^3(^2D)5p\ ^3D$ + 8 $4p^3(^2P)5p\ ^3D$
338 691.84	338 911	−219	3	60 $4p^3(^2D)5p\ ^1F$ + 27 $4p^3(^2D)5p\ ^3D$ + 6 $4p^3(^2P)5p\ ^3D$
339 930.18	340 026	−96	3	38 $4p^3(^2D)5p\ ^3D$ + 31 $4p^3(^2D)5p\ ^1F$ + 29 $4p^3(^2D)5p\ ^3F$

Notes. Energies are given in cm^{-1}. [(a)] From Sansonetti (2012). [(b)] This work. [(c)] Only the first three components that are larger than 5% are given.

Table A.10. continued.

E_{exp}[a]	E_{calc}[b]	ΔE	J	Leading components (in %) in LS coupling[c]
340 419.40	340 788	−369	4	99 $4p^3(^2D)5p\ ^3F$
343 583.26	343 764	−181	2	69 $4p^3(^2D)5p\ ^3P$ + 11 $4p^3(^2P)5p\ ^3P$ + 9 $4p^3(^4S)5p\ ^3P$
345 057.34	344 625	432	0	63 $4p^3(^2D)5p\ ^3P$ + 13 $4p^6\ ^1S$ + 11 $4s4p^4 4d\ ^1S$
345 344.22	345 367	−23	1	68 $4p^3(^2D)5p\ ^3P$ + 13 $4p^3(^2P)5p\ ^3S$ + 13 $4p^3(^4S)5p\ ^3P$
351 337.47	351 178	159	2	73 $4p^3(^2D)5p\ ^1D$ + 9 $4p^3(^2D)5p\ ^3P$ + 5 $4p^3(^2D)5p\ ^3F$
353 844.75	353 953	−108	1	70 $4p^3(^2P)5p\ ^3D$ + 17 $4p^3(^2P)5p\ ^1P$ + 6 $4p^3(^2D)5p\ ^3D$
356 566.83	356 544	23	2	76 $4p^3(^2P)5p\ ^3D$ + 9 $4p^3(^2P)5p\ ^3P$
357 247.90	356 846	402	1	72 $4p^3(^2P)5p\ ^3S$ + 17 $4p^3(^2D)5p\ ^3P$
357 554.36	357 640	−86	1	61 $4p^3(^2P)5p\ ^3P$ + 25 $4p^3(^2P)5p\ ^1P$ + 6 $4p^3(^2P)5p\ ^3D$
358 075.63	358 226	−150	0	89 $4p^3(^2P)5p\ ^3P$
359 646.95	359 681	−34	3	80 $4p^3(^2P)5p\ ^3D$ + 8 $4p^3(^2D)5p\ ^3F$ + 7 $4p^3(^2D)5p\ ^1F$
362 486.77	362 819	−332	2	75 $4p^3(^2P)5p\ ^1D$ + 9 $4p^3(^2D)5p\ ^1D$ + 6 $4p^3(^2D)5p\ ^3F$
363 332.24	363 543	−211	1	37 $4p^3(^2P)5p\ ^1P$ + 27 $4p^3(^2P)5p\ ^3P$ + 9 $4p^3(^2D)5p\ ^3D$
364 886.55	364 567	320	2	64 $4p^3(^2P)5p\ ^3P$ + 9 $4p^3(^2D)5p\ ^3P$ + 8 $4p^3(^2D)5p\ ^1D$
375 152.16	375 025	127	0	85 $4p^3(^2P)5p\ ^1S$ + 6 $4p^3(^2D)5p\ ^3P$
				Odd parity
154 032.29	154 076	−44	2	83 $4s4p^5\ ^3P$ + 11 $4p^3(^2D)4d\ ^3P$ + 5 $4p^3(^2P)4d\ ^3P$
160 017.52	160 034	−16	1	81 $4s4p^5\ ^3P$ + 11 $4p^3(^2D)4d\ ^3P$
164 015.68	163 939	77	0	83 $4s4p^5\ ^3P$ + 12 $4p^3(^2D)4d\ ^3P$
193 318.87	193 364	−45	1	59 $4s4p^5\ ^1P$ + 34 $4p^3(^2D)4d\ ^1P$
202 128.66	202 015	114	0	96 $4p^3(^4S)4d\ ^5D$
202 265.18	202 145	120	1	97 $4p^3(^4S)4d\ ^5D$
202 321.43	202 138	183	2	95 $4p^3(^4S)4d\ ^5D$
202 398.48	202 098	300	3	93 $4p^3(^4S)4d\ ^5D$
202 912.96	202 478	435	4	95 $4p^3(^4S)4d\ ^5D$
213 783.82	214 002	−218	2	28 $4p^3(^4S)4d\ ^3D$ + 27 $4p^3(^2D)4d\ ^3D$ + 21 $4p^3(^2D)4d\ ^3F$
216 104.17	216 941	−837	3	38 $4p^3(^2D)4d\ ^3D$ + 35 $4p^3(^4S)4d\ ^3D$ + 10 $4p^3(^2D)4d\ ^3F$
216 969.19	218 377	−1408	1	48 $4p^3(^2D)4d\ ^3D$ + 46 $4p^3(^4S)4d\ ^3D$
220 549.72	220 601	−51	2	53 $4p^3(^2D)4d\ ^3F$ + 20 $4p^3(^2D)4d\ ^3D$ + 13 $4p^3(^4S)4d\ ^3D$
221 778.44	224 869	−3091	0	94 $4p^3(^2D)4d\ ^1S$
222 368.34	222 178	190	3	63 $4p^3(^2D)4d\ ^3F$ + 12 $4p^3(^2P)4d\ ^3F$ + 12 $4p^3(^2D)4d\ ^3D$
224 844.36	224 311	533	4	67 $4p^3(^2D)4d\ ^3F$ + 14 $4p^3(^2P)4d\ ^3F$ + 13 $4p^3(^2D)4d\ ^3G$
229 949.55	228 812	1138	3	84 $4p^3(^2D)4d\ ^3G$ + 10 $4p^3(^2D)4d\ ^3F$
230 974.17	229 909	1065	4	71 $4p^3(^2D)4d\ ^3G$ + 24 $4p^3(^2D)4d\ ^3F$
232 585.90	231 483	1103	5	99 $4p^3(^2D)4d\ ^3G$
234 782.57	234 638	145	4	84 $4p^3(^2D)4d\ ^1G$ + 7 $4p^3(^2D)4d\ ^3G$
241 479.47	241 470	9	2	56 $4p^3(^2P)4d\ ^1D$ + 21 $4p^3(^2D)4d\ ^1D$ + 10 $4p^3(^2P)4d\ ^3F$
243 576.50	243 444	133	1	50 $4p^3(^2P)4d\ ^3D$ + 33 $4p^3(^2D)4d\ ^3D$ + 13 $4p^3(^4S)4d\ ^3D$
246 801.43	247 122	−321	0	64 $4p^3(^2P)4d\ ^3P$ + 28 $4p^3(^2D)4d\ ^3P$ + 5 $4p^3(^2D)4d\ ^1S$
248 011.88	247 969	43	1	68 $4p^3(^2P)4d\ ^3P$ + 20 $4p^3(^2D)4d\ ^3P$ + 5 $4p^3(^2D)4d\ ^3S$
248 383.31	248 528	−145	2	45 $4p^3(^2P)4d\ ^3D$ + 17 $4p^3(^2D)4d\ ^3D$ + 13 $4p^3(^2P)4d\ ^3F$
249 673.18	248 782	891	3	74 $4p^3(^2P)4d\ ^3F$ + 12 $4p^3(^2D)4d\ ^3F$ + 7 $4p^3(^2D)4d\ ^3G$
250 656.55	250 202	455	2	52 $4p^3(^2P)4d\ ^3F$ + 21 $4p^3(^2D)4d\ ^3F$ + 9 $4p^3(^2D)4d\ ^3D$
251 233.80	250 550	684	4	72 $4p^3(^2P)4d\ ^3F$ + 11 $4p^3(^2D)4d\ ^1G$ + 8 $4p^3(^2D)4d\ ^3G$
253 340.43	253 997	−657	3	39 $4p^3(^2P)4d\ ^3D$ + 32 $4p^3(^2D)4d\ ^3D$ + 12 $4p^3(^4S)4d\ ^3D$
255 118.53	255 358	−239	2	79 $4p^3(^2P)4d\ ^3P$ + 6 $4p^3(^2D)4d\ ^3P$ + 5 $4p^3(^2P)4d\ ^1D$
265 178.82	264 313	866	1	86 $4p^3(^2D)4d\ ^3S$ + 9 $4p^3(^2D)4d\ ^3P$
266 239.42	267 128	−889	3	53 $4p^3(^2P)4d\ ^1F$ + 20 $4p^3(^2D)4d\ ^1F$ + 20 $4p^3(^2P)4d\ ^3D$
266 325.33	266 051	274	2	67 $4p^3(^4S)5s\ ^5S$ + 20 $4p^3(^2D)4d\ ^3P$
267 351.03	267 752	−401	2	55 $4p^3(^2D)4d\ ^3P$ + 28 $4p^3(^4S)5s\ ^5S$ + 9 $4s4p^5\ ^3P$
269 614.82	269 237	378	1	32 $4p^3(^2D)4d\ ^3P$ + 26 $4p^3(^2D)4d\ ^1P$ + 17 $4s4p^5\ ^1P$
271 500.19	271 508	−8	3	40 $4p^3(^4S)4d\ ^3D$ + 25 $4p^3(^2P)4d\ ^3D$ + 16 $4p^3(^2D)4d\ ^3D$
274 951.74	275 050	−98	1	87 $4p^3(^4S)5s\ ^3S$
275 425.41	275 409	16	0	58 $4p^3(^2D)4d\ ^3P$ + 24 $4p^3(^2P)4d\ ^3P$ + 15 $4s4p^5\ ^3P$
275 488.13	275 748	−260	1	32 $4p^3(^2D)4d\ ^1P$ + 23 $4p^3(^2D)4d\ ^3P$ + 15 $4s4p^5\ ^1P$
276 821.46	276 811	10	2	31 $4p^3(^4S)4d\ ^3D$ + 31 $4p^3(^2P)4d\ ^3D$ + 15 $4p^3(^2D)4d\ ^3D$
280 067.09	280 014	53	1	40 $4p^3(^2P)4d\ ^3D$ + 33 $4p^3(^4S)4d\ ^3D$ + 15 $4p^3(^2D)4d\ ^3D$

Table A.10. continued.

E_{exp}[a]	E_{calc}[b]	ΔE	J	Leading components (in %) in LS coupling[c]
285 450.04	285 986	−536	2	59 $4p^3(^2D)4d\ ^1D$ + 20 $4p^3(^2P)4d\ ^1D$ + 7 $4p^3(^2P)4d\ ^3D$
288 831.62	288 867	−35	1	84 $4p^3(^2D)5s\ ^3D$ + 5 $4p^3(^2P)5s\ ^1P$
289 116.66	289 114	3	2	74 $4p^3(^2D)5s\ ^3D$ + 12 $4p^3(^2P)5s\ ^3P$ + 8 $4p^3(^2D)5s\ ^1D$
291 678.41	291 515	163	3	67 $4p^3(^2D)5s\ ^3D$ + 18 $4p^3(^2D)4d\ ^1F$ + 11 $4p^3(^2P)4d\ ^1F$
291 835.57	292 123	−287	3	39 $4p^3(^2D)4d\ ^1F$ + 31 $4p^3(^2D)5s\ ^3D$ + 21 $4p^3(^2P)4d\ ^1F$
294 818.15	294 792	26	2	82 $4p^3(^2D)5s\ ^1D$ + 13 $4p^3(^2D)5s\ ^3D$
306 075.40	305 775	300	1	73 $4p^3(^2P)4d\ ^1P$ + 10 $4p^3(^2P)5s\ ^3P$
306 607.40	306 678	−71	0	97 $4p^3(^2P)5s\ ^3P$
307 806.45	307 850	−44	1	73 $4p^3(^2P)5s\ ^3P$ + 10 $4p^3(^2P)4d\ ^1P$ + 10 $4p^3(^2P)5s\ ^1P$
311 699.75	311 767	−67	2	78 $4p^3(^2P)5s\ ^3P$ + 9 $4p^3(^2D)5s\ ^1D$ + 8 $4p^3(^2D)5s\ ^3D$
314 735.94	314 607	129	1	76 $4p^3(^2P)5s\ ^1P$ + 10 $4p^3(^2D)5s\ ^3D$ + 8 $4p^3(^2P)5s\ ^3P$
386 524.69	386 500	25	0	95 $4p^3(^4S)5d\ ^5D$
386 568.48	386 529	39	1	95 $4p^3(^4S)5d\ ^5D$
386 581.90	386 549	33	2	93 $4p^3(^4S)5d\ ^5D$
386 627.19	386 610	17	3	92 $4p^3(^4S)5d\ ^5D$
386 847.17	386 871	−24	4	94 $4p^3(^4S)5d\ ^5D$
391 772.82	391 786	−13	2	82 $4p^3(^4S)5d\ ^3D$ + 5 $4p^3(^2D)5d\ ^3D$
392 707.81	392 701	7	1	90 $4p^3(^4S)5d\ ^3D$
392 856.49	392 923	−67	3	88 $4p^3(^4S)5d\ ^3D$
402 356.59	402 373	−16	2	95 $4p^3(^4S)6s\ ^5S$
404 878.30	404 863	15	1	93 $4p^3(^4S)6s\ ^3S$
406 129.11	406 197	−68	2	76 $4p^3(^2D)5d\ ^3F$ + 7 $4p^3(^2P)5d\ ^3F$
407 282.42	407 438	−156	3	67 $4p^3(^2D)5d\ ^3F$ + 9 $4p^3(^2D)5d\ ^3G$ + 6 $4p^3(^2P)5d\ ^3F$
407 979.67	407 973	7	3	74 $4p^3(^2D)5d\ ^3G$ + 8 $4p^3(^2D)5d\ ^3F$ + 7 $4p^3(^2P)5d\ ^1F$
408 237.78	408 246	−8	4	55 $4p^3(^2D)5d\ ^3G$ + 30 $4p^3(^2D)5d\ ^1G$ + 13 $4p^3(^2P)5d\ ^3F$
408 586.08	408 454	132	1	56 $4p^3(^2D)5d\ ^3D$ + 23 $4p^3(^2D)5d\ ^1P$ + 5 $4p^3(^2P)5d\ ^3D$
410 365.34	410 412	−47	4	96 $4p^3(^2D)5d\ ^3F$
410 516.87	410 559	−42	2	52 $4p^3(^2D)5d\ ^3D$ + 24 $4p^3(^2D)5d\ ^3P$ + 9 $4p^3(^2P)5d\ ^3P$
411 152.84	411 157	−4	4	60 $4p^3(^2D)5d\ ^1G$ + 36 $4p^3(^2D)5d\ ^3G$
411 192.90	411 282	−89	5	100 $4p^3(^2D)5d\ ^3G$
411 800.14	411 849	−49	3	78 $4p^3(^2D)5d\ ^3D$ + 13 $4p^3(^2D)5d\ ^3F$
412 486.36	412 365	121	1	38 $4p^3(^2D)5d\ ^3S$ + 26 $4p^3(^2D)5d\ ^1P$ + 13 $4p^3(^2D)5d\ ^3P$
413 007.75	413 068	−60	2	44 $4p^3(^2D)5d\ ^3P$ + 34 $4p^3(^2D)5d\ ^3D$ + 11 $4p^3(^2D)5d\ ^1D$
413 446.26	413 461	−15	1	32 $4p^3(^2D)5d\ ^3P$ + 29 $4p^3(^2D)5d\ ^1P$ + 23 $4p^3(^2D)5d\ ^3D$
413 822.42	413 844	−22	0	85 $4p^3(^2D)5d\ ^3P$ + 9 $4p^3(^2D)5d\ ^1S$
414 775.09	414 672	103	1	46 $4p^3(^2D)5d\ ^3P$ + 41 $4p^3(^2D)5d\ ^3S$ + 11 $4p^3(^2D)5d\ ^1P$
415 542.33	415 304	238	2	65 $4p^3(^2D)5d\ ^1D$ + 19 $4p^3(^2D)5d\ ^3P$ + 6 $4p^3(^2D)5d\ ^3F$
417 657.82	417 714	−56	3	83 $4p^3(^2D)5d\ ^1F$
423 107.53	423 101	7	1	85 $4p^3(^2D)6s\ ^3D$ + 8 $4p^3(^2P)6s\ ^1P$
423 315.79	423 317	−1	2	64 $4p^3(^2D)6s\ ^3D$ + 20 $4p^3(^2D)6s\ ^1D$ + 13 $4p^3(^2P)6s\ ^3P$
426 317.28	426 300	17	3	98 $4p^3(^2D)6s\ ^3D$
427 207.25	427 185	22	2	25 $4p^3(^2P)5d\ ^3D$ + 25 $4p^3(^2D)6s\ ^1D$ + 23 $4p^3(^2P)5d\ ^3P$
427 217.06	427 268	−51	2	45 $4p^3(^2D)6s\ ^1D$ + 16 $4p^3(^2P)5d\ ^3D$ + 14 $4p^3(^2D)6s\ ^3D$
428 455.92	428 495	−39	1	57 $4p^3(^2P)5d\ ^3D$ + 29 $4p^3(^2P)5d\ ^3P$ + 7 $4p^3(^2P)5d\ ^1P$
430 001.70	430 034	−32	0	83 $4p^3(^2P)5d\ ^3P$ + 7 $4p^3(^2D)5d\ ^3P$ + 6 $4p^3(^2D)5d\ ^1S$
431 024.41	431 006	18	1	53 $4p^3(^2P)5d\ ^3P$ + 26 $4p^3(^2P)5d\ ^3D$ + 6 $4p^3(^2D)5d\ ^3S$
431 700.49	431 546	154	2	48 $4p^3(^2P)5d\ ^3P$ + 20 $4p^3(^2P)5d\ ^1D$ + 11 $4p^3(^2P)5d\ ^3D$
433 202.82	433 254	−51	3	58 $4p^3(^2P)5d\ ^3D$ + 11 $4p^3(^2P)5d\ ^3F$ + 10 $4p^3(^2P)5d\ ^1F$
433 660.35	433 473	187	3	70 $4p^3(^2P)5d\ ^1F$ + 11 $4p^3(^2P)5d\ ^3F$ + 9 $4p^3(^2D)5d\ ^3G$
433 958.19	434 057	−99	2	32 $4p^3(^2P)5d\ ^3D$ + 28 $4p^3(^2P)5d\ ^1D$ + 13 $4p^3(^2P)5d\ ^3F$
438 712.58	438 887	−174	1	75 $4p^3(^2P)5d\ ^1P$ + 6 $4p^3(^2P)5d\ ^3D$
441 606.30	441 607	−1	1	75 $4p^3(^2P)6s\ ^3P$ + 24 $4p^3(^2P)6s\ ^1P$
446 262.90	446 239	24	2	81 $4p^3(^2P)6s\ ^3P$ + 9 $4p^3(^2D)6s\ ^3D$ + 7 $4p^3(^2D)6s\ ^1D$
447 043.20	447 065	−22	1	64 $4p^3(^2P)6s\ ^1P$ + 19 $4p^3(^2P)6s\ ^3P$ + 14 $4p^3(^2D)6s\ ^3D$

Table A.11. Comparison between available experimental and calculated energy levels in Sr VI.

E_{exp} [a]	E_{calc} [b]	ΔE	J	Leading components (in %) in LS coupling[c]
				Odd parity
0.0	1	−1	1.5	93 $4p^3\ ^4S$
20 134.7	20 114	21	1.5	82 $4p^3\ ^2D$ + 13 $4p^3\ ^2P$
23 527.0	23 546	−19	2.5	97 $4p^3\ ^2D$
38 531.1	38 544	−13	0.5	97 $4p^3\ ^2P$
43 566.9	43 555	12	1.5	79 $4p^3\ ^2P$ + 15 $4p^3\ ^2D$
				Even parity
153 170.8	153 175	−4	2.5	90 $4s4p^4\ ^4P$ + 8 $4p^2(^3P)4d\ ^4P$
159 597.3	159 567	30	1.5	91 $4s4p^4\ ^4P$ + 8 $4p^2(^3P)4d\ ^4P$
162 238.2	162 269	−31	0.5	89 $4s4p^4\ ^4P$ + 8 $4p^2(^3P)4d\ ^4P$
188 319.4	188 458	−139	1.5	80 $4s4p^4\ ^2D$ + 13 $4p^2(^1D)4d\ ^2D$
189 978.4	189 846	132	2.5	81 $4s4p^4\ ^2D$ + 14 $4p^2(^1D)4d\ ^2D$
215 697.0	215 698	−1	1.5	60 $4s4p^4\ ^2P$ + 32 $4p^2(^3P)4d\ ^2P$
216 644.3	216 620	24	0.5	33 $4s4p^4\ ^2P$ + 42 $4s4p^4\ ^2S$ + 15 $4p^2(^3P)4d\ ^2P$
227 291.5	227 320	−29	0.5	41 $4s4p^4\ ^2S$ + 29 $4s4p^4\ ^2P$ + 18 $4p^2(^3P)4d\ ^2P$
327 320.0	327 321	−1	0.5	79 $4p^2(^3P)5s\ ^4P$ + 7 $4p^2(^3P)5s\ ^2P$ + 7 $4p^2(^1D)4d\ ^2S$
333 260.0	333 277	−17	1.5	93 $4p^2(^3P)5s\ ^4P$
338 240.0	338 259	−19	0.5	87 $4p^2(^3P)5s\ ^2P$ + 10 $4p^2(^3P)5s\ ^4P$
338 650.0	338 630	20	2.5	85 $4p^2(^3P)5s\ ^4P$ + 12 $4p^2(^1D)5s\ ^2D$
343 870.0	343 839	31	1.5	72 $4p^2(^3P)5s\ ^2P$ + 24 $4p^2(^1D)5s\ ^2D$
355 820.0	355 812	8	2.5	85 $4p^2(^1D)5s\ ^2D$ + 12 $4p^2(^3P)5s\ ^4P$
356 820.0	356 844	−24	1.5	74 $4p^2(^1D)5s\ ^2D$ + 22 $4p^2(^3P)5s\ ^2P$
378 990.0	378 990	0	0.5	91 $4p^2(^1S)5s\ ^2S$

Notes. Energies are given in cm^{-1}. [a] From Sansonetti (2012). [b] This work. [c] Only the first three components that are larger than 5% are given.

Table A.12. Comparison between available experimental and calculated energy levels in Sr VII.

E_{exp} [a]	E_{calc} [b]	ΔE	J	Leading components (in %) in LS coupling[c]
				Even parity
0	0	0	0	92 $4p^2\ ^3P$ + 5 $4p^2\ ^1S$
6845	6845	0	1	98 $4p^2\ ^3P$
12 545	12 545	0	2	82 $4p^2\ ^3P$ + 15 $4p^2\ ^1D$
28 490	28 490	0	2	82 $4p^2\ ^1D$ + 15 $4p^2\ ^3P$
51 814	51 814	0	0	91 $4p^2\ ^1S$ + 5 $4p^2\ ^3P$
				Odd parity
167 806	168 195	−389	1	85 $4s4p^3\ ^3D$ + 7 $4p4d\ ^3D$ + 5 $4s4p^3\ ^3P$
167 977	168 211	−234	2	83 $4s4p^3\ ^3D$ + 8 $4s4p^3\ ^3P$ + 7 $4p4d\ ^3D$
170 427	170 512	−85	3	92 $4s4p^3\ ^3D$ + 7 $4p4d\ ^3D$
190 425	190 379	46	0	92 $4s4p^3\ ^3P$ + 7 $4p4d\ ^3P$
191 215	191 034	181	1	86 $4s4p^3\ ^3P$ + 7 $4p4d\ ^3P$
192 193	191 749	444	2	76 $4s4p^3\ ^3P$ + 8 $4s4p^3\ ^3D$ + 7 $4p4d\ ^3P$
213 095	212 271	824	2	66 $4s4p^3\ ^1D$ + 25 $4p4d\ ^1D$ + 6 $4s4p^3\ ^3P$
232 870	232 675	195	1	77 $4s4p^3\ ^3S$ + 18 $4s4p^3\ ^1P$
247 754	248 567	−813	1	72 $4s4p^3\ ^1P$ + 19 $4s4p^3\ ^3S$ + 6 $4p4d\ ^1P$
373 400	373 402	−2	0	98 $4p5s\ ^3P$
374 670	374 668	2	1	78 $4p5s\ ^3P$ + 20 $4p5s\ ^1P$
386 270	386 270	0	2	98 $4p5s\ ^3P$
389 730	389 731	−1	1	78 $4p5s\ ^1P$ + 20 $4p5s\ ^3P$

Notes. Energies are given in cm^{-1}. [a] From Sansonetti (2012). [b] This work. [c] Only the first three components that are larger than 5% are given.

Table A.13. Comparison between available experimental and calculated energy levels in Te VI.

E_{exp} [a]	E_{calc} [b]	ΔE	J	Leading components (in %) in LS coupling[c]
				Even parity
0.0	0	0	0.5	99 $4d^{10}5s\ ^2S$
238 087.6	238 088	0	1.5	99 $4d^{10}5d\ ^2D$
239 736.2	239 736	0	2.5	99 $4d^{10}5d\ ^2D$
278 436.2	278 436	0	0.5	100 $4d^{10}6s\ ^2S$
480 834.0	480 935	−101	2.5	49 $4d^95p^2\ ^4D$ + 13 $4d^95p^2\ ^4F$ + 9 $4d^95p^2\ ^4P$
488 295.0	488 184	111	1.5	64 $4d^95p^2\ ^4D$ + 10 $4d^95p^2\ ^2D$ + 9 $4d^95p^2\ ^4F$
489 538.0	489 652	−114	0.5	56 $4d^95p^2\ ^2S$ + 19 $4d^95p^2\ ^2P$ + 8 $4d^95p^2\ ^4D$
490 499.0	490 411	88	1.5	59 $4d^95p^2\ ^2P$ + 12 $4d^95p^2\ ^2P$ + 8 $4d^95s5d\ ^2P$
498 636.0	498 676	−40	1.5	47 $4d^95p^2\ ^2D$ + 42 $4d^95p^2\ ^4F$ + 5 $4d^95p^2\ ^2P$
501 898.0	501 788	110	0.5	55 $4d^95p^2\ ^2P$ + 15 $4d^95p^2\ ^4P$ + 8 $4d^95s5d\ ^2P$
503 128.0	503 155	−27	1.5	42 $4d^95p^2\ ^4F$ + 31 $4d^95p^2\ ^2D$ + 5 $4d^95p^2\ ^4P$
504 027.0	503 990	37	2.5	32 $4d^95p^2\ ^4F$ + 24 $4d^95p^2\ ^4P$ + 19 $4d^95p^2\ ^2F$
506 535.0	506 525	10	1.5	49 $4d^95p^2\ ^2D$ + 34 $4d^95p^2\ ^4P$ + 8 $4d^95s5d\ ^2D$
510 691.0	510 671	20	2.5	52 $4d^95p^2\ ^2D$ + 30 $4d^95p^2\ ^2D$ + 7 $4d^95s5d\ ^2D$
511 382.0	511 487	−105	0.5	86 $4d^95p^2\ ^2P$ + 6 $4d^95p^2\ ^2S$
513 098.0	512 913	185	1.5	53 $4d^95p^2\ ^2P$ + 19 $4d^95p^2\ ^2P$ + 8 $4d^95p^2\ ^2D$
517 679.0	517 850	−171	2.5	43 $4d^95p^2\ ^2F$ + 13 $4d^95p^2\ ^2D$ + 10 $4d^95p^2\ ^2F$
				Odd parity
93 334.6	93 335	0	0.5	99 $4d^{10}5p\ ^2P$
105 150.2	105 150	0	1.5	99 $4d^{10}5p\ ^2P$
314 198.4	314 198	0	0.5	100 $4d^{10}6p\ ^2P$
318 601.4	318 601	0	1.5	100 $4d^{10}6p\ ^2P$
376 310.0	376 297	13	1.5	58 $4d^95s5p\ ^4P$ + 18 $4d^95s5p\ ^4D$ + 12 $4d^95s5p\ ^2P$
385 045.0	385 062	−17	0.5	75 $4d^95s5p\ ^4P$ + 13 $4d^95s5p\ ^4D$ + 11 $4d^95s5p\ ^2P$
388 165.0	388 165	0	1.5	44 $4d^95s5p\ ^2D$ + 19 $4d^95s5p\ ^4P$ + 14 $4d^95s5p\ ^2P$
392 650.0	392 682	−32	1.5	56 $4d^95s5p\ ^2P$ + 22 $4d^95s5p\ ^4D$ + 10 $4d^95s5p\ ^2P$
393 730.0	393 708	22	0.5	63 $4d^95s5p\ ^2P$ + 23 $4d^95s5p\ ^2P$ + 7 $4d^95s5p\ ^4D$
400 015.0	400 008	7	1.5	52 $4d^95s5p\ ^4D$ + 20 $4d^95s5p\ ^2D$ + 10 $4d^95s5p\ ^4P$
411 220.0	411 227	−7	1.5	60 $4d^95s5p\ ^2P$ + 32 $4d^{10}7p\ ^2P$
422 875.0	422 864	11	0.5	75 $4d^95s5p\ ^2P$ + 21 $4d^95s5p\ ^2P$

Notes. Energies are given in cm^{-1}. [a] From Crooker & Joshi (1964), Dunne & O'Sullivan (1992), and Ryabtsev et al. (2007). [b] This work. [c] Only the first three components larger than 5% are given.

Table A.14. Comparison between available experimental and calculated energy levels in I VI.

E_{exp} [a]	E_{calc} [b]	ΔE	J	Leading components (in %) in LS coupling[c]
				Even parity
0.0	0	0	0	98 $5s^2\ ^1S$
200 084.8	199 954	131	0	91 $5p^2\ ^3P$ + 9 $5p^2\ ^1S$
208 474.5	208 663	−188	1	100 $5p^2\ ^3P$
209 431.7	209 483	−51	2	54 $5p^2\ ^1D$ + 32 $5p^2\ ^3P$ + 13 $5s5d\ ^1D$
221 983.8	221 854	130	2	67 $5p^2\ ^3P$ + 23 $5p^2\ ^1D$ + 10 $5s5d\ ^1D$
245 658.5	245 671	−12	0	87 $5p^2\ ^1S$ + 9 $5p^2\ ^3P$
251 816.9	251 813	4	1	99 $5s5d\ ^3D$
252 540.3	252 548	−8	2	99 $5s5d\ ^3D$
253 751.8	253 749	3	3	99 $5s5d\ ^3D$
270 094.7	270 103	−8	2	73 $5s5d\ ^1D$ + 21 $5p^2\ ^1D$
296 253.4	296 253	0	1	100 $5s6s\ ^3S$
302 858.0	302 858	0	0	100 $5s6s\ ^1S$
416 535.0	416 535	0	1	100 $5s7s\ ^3S$
418 707.0	418 707	0	0	100 $5s7s\ ^1S$

Notes. Energies are given in cm^{-1}. [a] From Tauheed et al. (1997). [b] This work. [c] Only the first three components larger than 5% are given.

Table A.14. continued.

E_{exp}[a]	E_{calc}[b]	ΔE	J	Leading components (in %) in LS coupling[c]
				Odd parity
85 665.6	85 709	−43	0	100 5s5p ^{3}P
89 261.7	89 206	56	1	97 5s5p ^{3}P
99 685.4	99 694	−9	2	100 5s5p ^{3}P
127 423.8	127 425	−1	1	95 5s5p ^{1}P
335 737.6	335 685	53	0	98 5s6p ^{3}P
336 197.2	336 250	−53	1	80 5s6p ^{3}P + 18 5s6p ^{1}P
340 462.4	340 471	−9	2	97 5s6p ^{3}P
341 729.0	341 715	14	1	78 5s6p ^{1}P + 18 5s6p ^{3}P
347 472.0	347 424	48	2	79 5p5d ^{3}F + 17 5p5d ^{1}D
353 652.0	353 515	137	3	89 5p5d ^{3}F + 6 5p5d ^{3}D
356 797.0	356 664	133	2	52 5p5d ^{1}D + 21 5p5d ^{3}P + 14 5p5d ^{3}D
361 780.0	362 087	−307	1	71 5p5d ^{3}D + 20 5p5d ^{3}P + 7 5p5d ^{1}P
362 500.0	362 198	302	4	97 5p5d ^{3}F
366 578.0	366 655	−77	2	38 5p5d ^{3}D + 28 5p5d ^{1}D + 25 5p5d ^{3}P
371 695.0	371 764	−69	3	89 5p5d ^{3}D + 7 5p5d ^{3}F
373 009.0	373 262	−253	0	98 5p5d ^{3}P
373 131.0	373 343	−212	1	75 5p5d ^{3}P + 23 5p5d ^{3}D
373 476.0	373 534	−58	2	51 5p5d ^{3}P + 45 5p5d ^{3}D
387 975.0	387 436	539	3	62 5p5d ^{1}F + 29 5s5f ^{1}F
402 785.0	402 622	163	0	98 5p6s ^{3}P
404 136.0	404 309	−173	1	78 5p6s ^{3}P + 17 5p6s ^{1}P
417 041.0	417 074	−33	2	98 5p6s ^{3}P
419 603.0	419 555	48	1	61 5p6s ^{1}P + 18 5p6s ^{3}P + 16 5s7p ^{1}P

Table A.15. Calculated HFR oscillator strengths ($\log g_i f_{ik}$) and transition probabilities ($g_k A_{ki}$) in Se V.

	Lower level			Upper level					
Wavelength[a]/Å	energy[b]/cm^{-1}	parity	J	energy[b]/cm^{-1}	parity	J	$\log g_i f_{ik}$	$g_k A_{ki}$/s^{-1}	CF

Notes. CF is the absolute value of the cancellation factor as defined by Cowan (1981). In Cols. 3 and 6, e represents even and o odd. [(a)] All wavelengths (given in vacuum for $\lambda < 2000$ Å, air for 2000 Å $\leq \lambda \leq$ 20 000 Å, vacuum for 20 000 Å $< \lambda$) are deduced from experimental energy levels. [(b)] Experimental energy levels taken from Churilov & Joshi (1995).

Table A.16. Calculated HFR oscillator strengths ($\log g_i f_{ik}$) and transition probabilities ($g_k A_{ki}$) in Sr IV.

	Lower level			Upper level					
Wavelength[a]/Å	energy[b]/cm^{-1}	parity	J	energy[b]/cm^{-1}	parity	J	$\log g_i f_{ik}$	$g_k A_{ki}$/s^{-1}	CF

Notes. CF is the absolute value of the cancellation factor as defined by Cowan (1981). In Cols. 3 and 6, e represents even and o odd. [(a)] All wavelengths (given in vacuum for $\lambda < 2000$ Å, air for 2000 Å $\leq \lambda \leq$ 20 000 Å, vacuum for 20 000 Å $< \lambda$) are deduced from experimental energy levels. [(b)] Experimental energy levels taken from Sansonetti (2012).

Table A.17. Calculated HFR oscillator strengths ($\log g_i f_{ik}$) and transition probabilities ($g_k A_{ki}$) in Sr V.

	Lower level			Upper level					
Wavelength[a]/Å	energy[b]/cm^{-1}	parity	J	energy[b]/cm^{-1}	parity	J	$\log g_i f_{ik}$	$g_k A_{ki}$/s^{-1}	CF

Notes. CF is the absolute value of the cancellation factor as defined by Cowan (1981). In Cols. 3 and 6, e represents even and o odd. [(a)] All wavelengths (given in vacuum for $\lambda < 2000$ Å, air for 2000 Å $\leq \lambda \leq$ 20 000 Å, vacuum for 20 000 Å $< \lambda$) are deduced from experimental energy levels. [(b)] Experimental energy levels taken from Sansonetti (2012).

Table A.18. Calculated HFR oscillator strengths ($\log g_i f_{ik}$) and transition probabilities ($g_k A_{ki}$) in Sr VI.

	Lower level			Upper level					
Wavelength[a]/Å	energy[b]/cm^{-1}	parity	J	energy[b]/cm^{-1}	parity	J	$\log g_i f_{ik}$	$g_k A_{ki}$/s^{-1}	CF

Notes. CF is the absolute value of the cancellation factor as defined by Cowan (1981). In Cols. 3 and 6, e represents even and o odd. [(a)] All wavelengths (given in vacuum for $\lambda < 2000$ Å, air for 2000 Å $\leq \lambda \leq$ 20 000 Å, vacuum for 20 000 Å $< \lambda$) are deduced from experimental energy levels. [(b)] Experimental energy levels taken from Sansonetti (2012).

Table A.19. Calculated HFR oscillator strengths ($\log g_i f_{ik}$) and transition probabilities ($g_k A_{ki}$) in Sr VII.

	Lower level			Upper level					
Wavelength[a]/Å	energy[b]/cm^{-1}	parity	J	energy[b]/cm^{-1}	parity	J	$\log g_i f_{ik}$	$g_k A_{ki}$/s^{-1}	CF

Notes. CF is the absolute value of the cancellation factor as defined by Cowan (1981). In Cols. 3 and 6, e represents even and o odd. [(a)] All wavelengths (given in vacuum for $\lambda < 2000$ Å, air for 2000 Å $\leq \lambda \leq$ 20 000 Å, vacuum for 20 000 Å $< \lambda$) are deduced from experimental energy levels. [(b)] Experimental energy levels taken from Sansonetti (2012).

Table A.20. Calculated HFR oscillator strengths ($\log g_i f_{ik}$) and transition probabilities ($g_k A_{ki}$) in Te VI. CF is the absolute value of the cancellation factor as defined by Cowan (1981).

	Lower level			Upper level					
Wavelength[a]/Å	energy[b]/cm^{-1}	parity	j	energy[b]/cm^{-1}	parity	j	$\log g_i f_{ik}$	$g_k A_{ki}$/s^{-1}	CF

Notes. In Cols. 3 and 6, e represents even and o odd. [(a)] All wavelengths (given in vacuum for $\lambda < 2000$ Å, air for 2000 Å $\leq \lambda \leq$ 20 000 Å, vacuum for 20 000 Å $< \lambda$) are deduced from experimental energy levels. [(b)] Experimental energy levels taken from Crooker & Joshi (1964), Dunne & O'Sullivan (1992), and Ryabtsev et al. (2007).

Table A.21. Calculated HFR oscillator strengths ($\log g_i f_{ik}$) and transition probabilities ($g_k A_{ki}$) in I VI.

	Lower level			Upper level					
Wavelength[a]/Å	energy[b]/cm^{-1}	parity	j	energy[b]/cm^{-1}	parity	J	$\log g_i f_{ik}$	$g_k A_{ki}$/s^{-1}	CF

Notes. CF is the absolute value of the cancellation factor as defined by Cowan (1981). In Cols. 3 and 6, e represents even and o odd. [(a)] All wavelengths (given in vacuum for $\lambda < 2000$ Å, air for 2000 Å $\leq \lambda \leq$ 20 000 Å, vacuum for 20 000 Å $< \lambda$) are deduced from experimental energy levels. [(b)] Experimental energy levels taken from Tauheed et al. (1997).

Appendix B: Additional figure

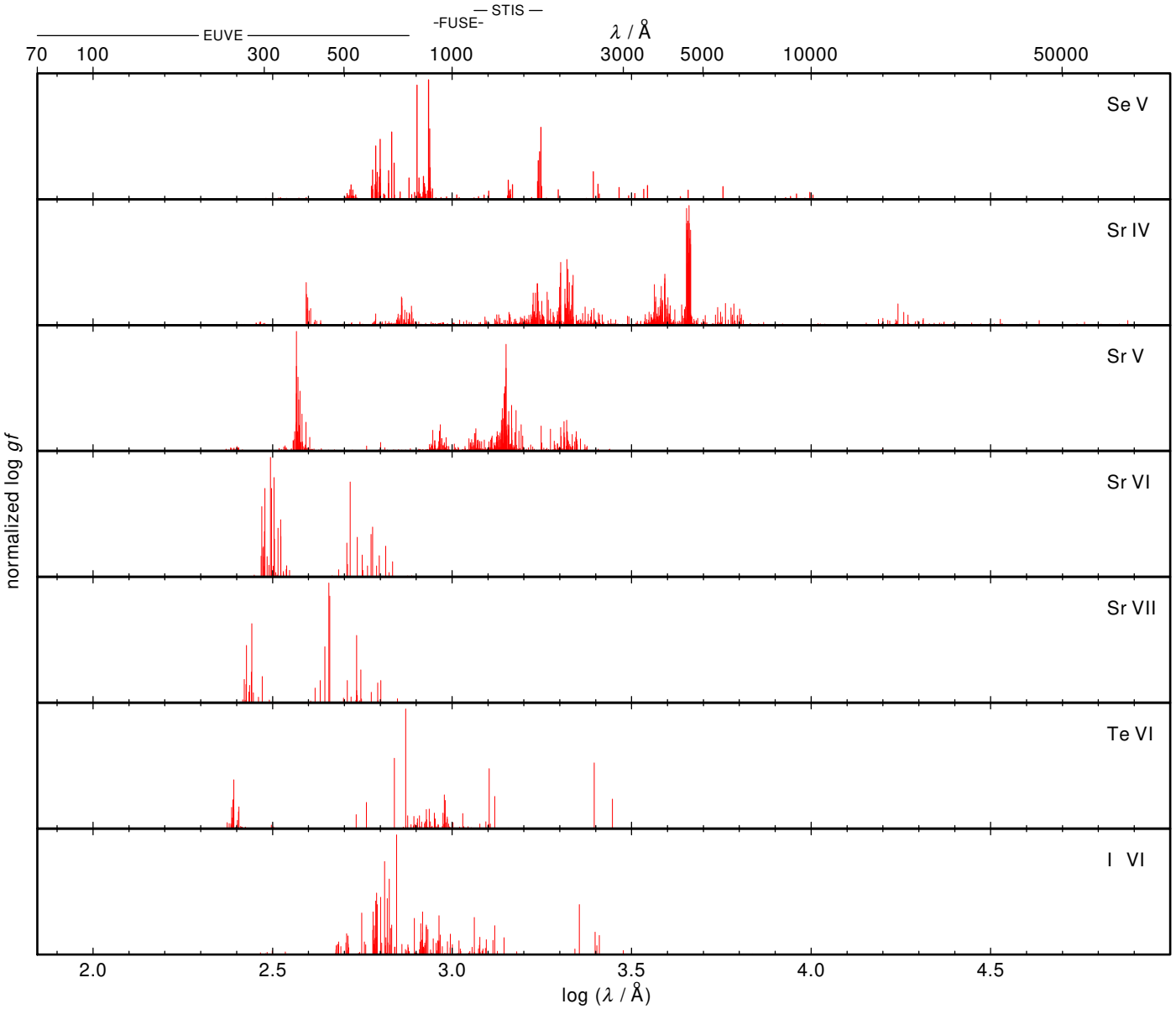

Fig. B.1. Newly calculated $\log g_i f_{ik}$ values of Se V, Sr IV–VII, Te VI, and I VI (*from top to bottom*). The $\log g_i f_{ik}$ values are normalized to the strongest line, matching 95% of the panels' heights. The wavelength ranges of EUVE and of our FUSE and STIS spectra are indicated at the top.